Journal of Thermal Analysis Vol. 50 (1997) 279-333

Dedicated to Prof. Menachem Steinberg on the occasion of his 65th birthday

A MATHEMATICAL MODEL FOR MODULATED DIFFERENTIAL SCANNING CALORIMETRY

A. A. Lacey[1], *C. Nikolopoulos*[1] *and M. Reading*[2]

[1]Department of Mathematics, Heriot-Watt University, Riccarton,
Edinburgh, EH14 4AS
[2]ICI Paints, Wexham Road, Slough, Berks, SL2 5DS, UK

Abstract

Reading and co-workers introduced a new technique a few years ago called Modulated Differential Scanning Calorimetry or MDSC. Here the first part of a theoretical analysis for this technique is given. A simple mathematical model for modulated differential scanning calorimetry in the form of an ordinary differential equation is derived. The model is analysed to find the effect of a kinetic event in the form of a chemical reaction. Some possible sources of error are discussed. A more sophisticated version of the model allowing for spatial variation in a calorimeter is developed and it is seen how it can be reduced to the earlier model. Some preliminary work on a phase change is also presented.

Keywords: mathematical model, MDSC

1. Introduction

A few years ago a new method was introduced by Reading and collaborators called Modulated Differential Scanning Calorimetry or MDSC [1–4]. In this method a conventional DSC is used with the modification that the conventional isothermal or linear rising temperature programme is modulated by a perturbation. The resultant signal is then analyzed using a combination of an averaging process and a Fourier transform to deconvolute the sample's response to the underlying ramp from its response to the modulation which can then give rise to an underlying and a cyclic heat capacity [1–4]. The cyclic heat capacity can be divided into a signal that is in phase (with dT/dt) and a component that is out of phase (with dT/dt) [1, 3]. Reading has also proposed that it is useful to derive a fourth signal called the non-reversing component by subtracting the in-phase part of the cyclic heat capacity from the underlying heat capacity. These quantities can be expressed as heat flows [1] or heat capacities [3]. The need for a rigorous theoretical analysis of the response of a typical non-ideal calorimeter un-

0368–4466/97/ $ 5.00

John Wiley & Sons Limited
Chichester

der modulated conditions in order that instrumental factors can be accounted for by calibration has been pointed out [2, 3]. Here we present the first part of this analysis. Because the term Modulated DSC has become proprietary we now recommend the name Modulated-Temperature DSC or MTDSC.

We start, in Section 2, by deriving an ordinary differential equation (ODE) model for Modulated Temperature Differential Scanning Calorimetry (MTDSC). The model is essentially that discussed in [5–8]. Here cases where the sample undergoes a chemical reaction are considered and it is shown how MTDSC can be used to obtain better values for specific heats than are possible with conventional differential scanning calorimetry.

Section 3 discusses possible sources of error due to the separation of measurement into the "underlying" and "cyclic" parts. The error is found to be small if the frequency used is high in comparison with rates of change of quantities of interest.

In Section 4 more accurate models, with the calorimeter being considered one-dimensional and then three-dimensional, are obtained. It is seen that the procedure used for the ODE model remains valid and that these more complicated models can be reduced to the ODE version for sufficiently large periods.

Finally, the effect of having a sample which changes phase is briefly considered. Three possible models are discussed. The first has proportion of each phase dependent only upon temperature, in the second the proportion obeys some differential equation (like a chemical-reaction model), and the third is a Stefan-like model with a sharp interface between the two phases.

2. Ordinary differential equation model

The simplest representation of the differential scanning calorimeter is a discrete (in space) model, with the sample and reference pans taking the temperatures $T_s(t)$ and $T_R(t)$, respectively. The rates of heat transfer between the pans and heat source are proportional to the temperature differences. A fuller model, allowing for temperature variation within the calorimeter and for heat content of the calorimeter, is discussed in a later section.

To start with it is assumed that the pans' temperatures are measured precisely but at the end of this section this assumption is dropped. Likewise the calorimeter is generally taken to be unbiased (symmetric).

2.1 The model

The model obtained here is essentially that appearing in [5–8]. For both pans having a heat capacity C_R, the reference pan being empty but the sample pan containing a specimen with heat capacity C_s, the rates of temperature change and heat flows are related by

$$(C_R + C_s)\frac{\mathrm{d}T_s}{\mathrm{d}t} + f = \frac{\mathrm{d}Q_s}{\mathrm{d}t_s}, \quad C_R\frac{\mathrm{d}T_R}{\mathrm{d}t} = \frac{\mathrm{d}Q_R}{\mathrm{d}t_R} \tag{1}$$

where f is the rate of absorption of heat by any kinetic event (phase transition, chemical reaction etc.); of course $f>0$ and $f<0$ for endothermic and exothermic cases respectively. (The equations are easily modified to account for any material that the reference pan might contain.)

The rates of heat transfer are simply

$$\frac{\mathrm{d}Q_s}{\mathrm{d}t_s} = K_o(T_F - T_s) + K_1(T_R - T_s) \tag{2}$$

and

$$\frac{\mathrm{d}Q_R}{\mathrm{d}t_R} = K_o(T_F - T_R) + K_1(T_s - T_R),$$

using the symmetry assumption in writing down identical heat transfer coefficients. Then, on writing

$$\Delta T = T_R - T_s,$$

the measured temperature difference, the difference of Eqs (2) gives, on applying (1),

$$C_R\frac{\mathrm{d}\Delta T}{\mathrm{d}t} + K\Delta T = C_s\frac{\mathrm{d}T_s}{\mathrm{d}t} + f, \tag{3}$$

where $K=K_o+2K_1$.

Note that allowing for heat transfer to and from the environment by including terms $K_2(T_e-T_s)$ and $K_2(T_e-T_R)$ in (2) results in (3) with K changed to $K_o+2K_1+K_2$.

(It is also possible to include other discrete heat capacities to try to represent parts of the calorimeter itself. The study of the more complicated system follows in a similar manner and leads to similar results.)

For modulated-temperature differential scanning calorimetry (MTDSC) T_s is prescribed to be

$$T_s = T_o + bT + B\sin\omega t, \tag{4}$$

for an initial temperature T_o, ramp b, amplitude of oscillation B, and angular frequency ω. Of course this control of T_s is done via adjusting the temperature of the furnace, T_F. Equation (4) essentially defines the phase through the convention that the sinusoidal part is indeed $\sin\omega t$. Then

$$C_R\frac{\mathrm{d}\Delta T}{\mathrm{d}t} + K\Delta T = C_s b + BC_s\omega\cos\omega t + f. \tag{5}$$

2.2 The inert case

If the sample is inert (which should ideally be the case for calibration) $f \equiv 0$,

$$C_R\frac{d\Delta T}{dt} + K\Delta T = C_s b + B\omega C_s \cos\omega t,$$

and

$$\Delta T = \frac{C_s b}{K}(1 - e^{-Kt/C_R}) + \frac{C_s B\omega}{K^2 + \omega^2 C_R^2}(K\cos\omega t + \omega C_R \sin\omega t - Ke^{-Kt/C_R}).$$

This solution only applies exactly if K, C_s, ... are all constant but we shall see later (§2.4 and Section 3) something very similar applies even if they vary with temperature.

The transient terms (those evolving e^{-Kt/C_R}) are included to ensure that $\Delta T=0$ at $t=0$ ($T_R=T_s=T_0$ initially) but for cases of interest C_R/K is large compared to run times (and event times) and these exponentials can be neglected to give the steadily oscillating temperature difference

$$\begin{aligned}\Delta T &= \frac{C_s b}{K} + \frac{C_s B\omega}{K^2 + \omega^2 C_R^2}(K\cos\omega t + \omega C_R \sin\omega t)\\ &= \frac{C_s b}{K} + \frac{C_s B\omega}{\sqrt{K^2 + \omega^2 C_R^2}}\cos(\omega t - \varphi) = \overline{\Delta T} + \widetilde{\Delta T},\end{aligned} \tag{6}$$

separating the signal into its underlying $\overline{\Delta T}$ and cyclic $\widetilde{\Delta T}$ parts [4–6, 9].

The underlying measurement of heat capacity is seen to be

$$\bar{C}_s = \frac{K}{b}\overline{\Delta T} \tag{7}$$

and, on writing

$$|\widetilde{\Delta T}| = \max\widetilde{\Delta T} = \frac{C_s B\omega}{\sqrt{K^2 + \omega^2 C_R^2}},$$

the cyclic (amplitude) measurement is

$$\tilde{C}_s = \frac{\sqrt{K^2 + \omega^2 C_R^2}}{B\omega}|\widetilde{\Delta T}|. \tag{8}$$

The constants C_R and K that appear in (7) and (8) can be determined by calibration using a sample of known heat capacity.

The phase lag φ is given by

$$\varphi = \varphi_b \equiv \tan^{-1}\frac{\omega C_R}{K}, \tag{9}$$

and, for the this simple case, does not give any information about C_s but instead relates C_R and K. It should be emphasized that this phase difference is between the cyclic parts $\widetilde{\Delta T}$ and $\mathrm{d}\widetilde{T}_s/\mathrm{d}t$ of ΔT and $\mathrm{d}T_s/\mathrm{d}t$. If some other signal, such as the heat source, is used in determining sine and cosine components of $\widetilde{\Delta T}$ there will be an additional contribution to the phase: $\widetilde{\Delta T} = |\widetilde{\Delta T}| \cos(\omega t - \varphi_b - \varphi_s)$ for $T_s = T_0 + bt + B\sin(\omega t - \varphi_s)$.

The phase lag can be thought of as a measure of how far from "ideal" the calorimeter is. For $\varphi \ll 1$, that is $\omega C_R \ll K$,

$$\widetilde{\Delta T} \cong \frac{\omega B C_s}{K}\cos\omega t$$

so that the temperature difference is in phase with the rate of change of temperature, $\mathrm{d}T_s/\mathrm{d}t$. There is then a direct correspondence between heat flow and temperature difference, $\mathrm{d}Q_s/\mathrm{d}t = K\Delta T$, and the cyclic signal can be used in a similar manner to the underlying signal:

$$\text{heat capacity} = \frac{K \times (\text{maximum})\ \text{temperature difference}}{(\text{maximum})\ \text{rate of temperature rise}}. \tag{10}$$

With φ not small the right hand side of (10) could be multiplied by $\sec\varphi = \sqrt{1 + \frac{\omega^2 C_R^2}{K^2}}$ to give the correct value as in (8). Of course the only important quantity is the product $K \sec\varphi$ which can be found by calibration.

In practical terms these results mean that an MTDSC instrument can be simply calibrated by using a material of known heat capacity such as sapphire. This procedure is illustrated in [3]. It also means that the phase lag for an inert case will have some value which is a function of the prooperties of the calorimeter and will usually not be zero. It will also change as a function of temperature thus providing a baseline. We shall see later, Section 2.4, that deviations from this baseline arise as a consequence of transitions and that these deviations can be used to calculate the in and out of phase cyclic components as illustrated in [1].

2.3 A chemical reaction

In the event of a first-order chemical reaction occurring the fraction a of some agent decays according to

$$\frac{\mathrm{d}a}{\mathrm{d}t} = -ag(T_s), \tag{11}$$

where $g(T)$ is typically of Arrhenius type, say

$$g(T)=A\mathrm{e}^{-E/RT}. \tag{12}$$

With $T_s=T_0+bt+B\sin\omega t$ and $a(0)=a_0$=initial fraction,

$$a=a_0\exp\left[-\int_0^t g(T_0+bt_1+B\sin\omega t_1)\mathrm{d}t_1\right]. \tag{13}$$

If the amplitude B is small enough g can be linearized and (13) simplifies:

$$a\cong a_0\exp\left[-\int_0^t g(T_0+bt_1)\mathrm{d}t_1-B\int_0^t g'(T_0+bt_1)\sin\omega t_1\mathrm{d}t_1\right]$$

$$\cong a_0\exp\left[-\int_0^t g(T_0+bt_1)\mathrm{d}t_1\right]\left[1-B\int_0^t g'(T_0+bt_1)\sin\omega t_1\mathrm{d}t_1\right]$$

$$=\bar{a}+\tilde{a},$$

where the underlying fraction is (approximately)

$$\bar{a}=a_0\exp\left[-\int_0^t g(T_0+bt_1)\mathrm{d}t_1\right] \tag{14}$$

and the cyclic fraction is

$$\tilde{a}=-B\bar{a}\int_0^t g'(T_0+bt_1)\sin\omega t_1\mathrm{d}t_1$$

(For an p-th order reaction with $p\neq 1$ (14) is replaced by

$$\bar{a}=a_0\left[1+(p-1)a_0^{p-1}\int_0^t g\mathrm{d}t_1\right]^{-1/(p-1)}.)$$

It should be noted that this linearization clearly holds if $Bg'\ll g$ ($'$ here meaning $\mathrm{d}/\mathrm{d}T$), so quantities change by relatively small amounts over half a cycle and $B\int_0^t g'\sin\omega t_1\mathrm{d}t_1\ll 1$. For an Arrhenius law, (12), these require that $BE/RT^2\ll 1$ and $BAE\mathrm{e}^{-E/RT}/RT^2\omega\ll 1$. (Even if these fail to hold linearization can give reasonable approximations. Certainly experimental observations are consistent with a linear response. Taking values $E=10^5$ J mol^{-1}, $T\cong\Delta 300$ K, $A\cong 10^4$ s^{-1}, $\omega=10^{-1}$ s^{-1}, and B=1 K, the validity of linearization is clear: $BE/RT^2 \cong 10^{-1}$ while $BAEe^{-E/RT}/RT^2\omega \cong 10^{-9}$.)

The rate of heat taken up by an endothermic reaction with heat of reaction H is then, on continuing to linearize,

$$f = -HM\frac{\mathrm{d}a}{\mathrm{d}t}g(T_s)$$

$$\cong HM\left\{g(t_o + bt)\bar{a} + B\left[g'(T_o + bt)\sin\omega t - g(T_o + bt)\int_0^t g'(T_o + bt_1)\sin\omega t_1 \mathrm{d}t_1\right]\bar{a}\right\}, \quad (15)$$

for a sample of mass M.

Substituting the expression (15) into the differential Eq. (5) and solving leads to

$$\Delta T = \frac{C_s b}{K}(1 - e^{-KT/C_R}) + \frac{HM}{C_R}\int_0^t e^{K(s-t)/C_R}\,\bar{a}(s)g(T_o + bs)\mathrm{d}s$$
$$+ \frac{C_s B\omega}{K^2 + \omega^2 C_R^2}(K\cos\omega t + \omega C_R \sin\omega t - Ke^{-Kt/C_R}) \quad (16)$$
$$+ \frac{HMB}{C_R}\int_0^t e^{-K(s-t)/C_R}\,\bar{a}(s)\left[g'(T_o + bs)\sin\omega s - g(T_o + bs)\int_0^s g'(T_o + bt_1)\sin\omega t_1)\mathrm{d}t_1\right]\mathrm{d}s$$

which is not immediately useful.

To get a more helpful equation for ΔT the right-hand side has to be approximated, which in turn demands that small terms must be identified and neglected. To this end the variables are scaled: $T=T_1\theta$, with T_1 a typical absolute temperature, such as that at the end of an experiment; $t=T_1\tau/b$, since T_1/b is of the size of the duration of an experiment (it is assumed that T_o is not close to T_1 and the events last for the same sort of time) and $a=a_o\alpha$.

Then

$$\bar{\alpha} = \exp\left[-\int_0^\tau \frac{T_1 g}{b}\mathrm{d}\tau_1\right] \quad (17)$$

and

$$\tilde{\alpha} = -\frac{B}{b}\int_0^\tau \frac{\mathrm{d}g}{\mathrm{d}\theta}\sin\Omega\tau_1 \mathrm{d}\tau_1 \quad (18)$$

where $\Omega = \omega T_1/b$.

It is normal for a large number of oscillations to occur during any one event (so that the decomposition into underlying and cyclic parts makes sense): $\Omega \gg 1$. Integrating (18) by parts then gives

$$\tilde{\alpha} = \frac{B\bar{\alpha}}{b\Omega}\left(\frac{\mathrm{d}g}{\mathrm{d}\theta}\cos\Omega\tau - \left.\frac{\mathrm{d}g}{\mathrm{d}\theta}\right|_{0}\right), \tag{19}$$

provided that

$$\frac{1}{\Omega}\frac{\mathrm{d}^2g}{\mathrm{d}\theta^2} \ll \frac{\mathrm{d}g}{\mathrm{d}\theta} \tag{20}$$

(rapid oscillations dominate any sensitive temperature dependence). The second term of (19) can be absorbed into the underlying $\bar{\alpha}$ and neglected if $\frac{B}{b\Omega}\frac{\mathrm{d}g}{\mathrm{d}\theta} \ll 1$. Now

$$f \cong HVa_{0}\tilde{\alpha}\left\{g + \frac{B}{T_1}\left(\frac{\mathrm{d}g}{\mathrm{d}\theta}\sin\Omega\tau + \frac{T_1}{b\Omega}\frac{\mathrm{d}g}{\mathrm{d}\theta}g\cos\Omega\tau\right)\right\}$$

$$\cong HVa_{0}\bar{\alpha}\left(g + \frac{B}{T_1}\frac{\mathrm{d}g}{\mathrm{d}\varphi}\sin\Omega\tau\right) = \bar{f} + \tilde{f}$$

if $\frac{T_1}{b\Omega}g \ll 1$.

Figure 1 illustrates the form of underlying ($\bar{f}$) and cyclic ($\tilde{f}$) parts as well as the full rate of heat absorption f, taking the not necessarily accurate values $T_0=300$ K, $b=0.2$ K s^{-1}, $\omega=0.063$ s^{-1}, $B=7.5$ K, $R=8.3$ J K^{-1} mol^{-1}, $E=10^5$ J mol^{-1}, $A=10^3$ s^{-1}, $H=10^4$ J kg^{-1}, $a_0=0.95$, $M=10^{-5}$ kg, $C_R=0.1$ J K^{-1}, $K=850$ W K^{-1} and $C_s=0.024$ J K^{-1}.

With the Arrhenius law $g(T)=A\mathrm{e}^{-E/RT}$ the assumption needed are valid if

$$\frac{BE}{RT^2} \ll 1,\quad \frac{BE}{RT}\times\frac{A\mathrm{e}^{-E/RT}}{b\Omega} \ll 1,\quad \Omega \gg 1,\quad \frac{RT\Omega}{E} \gg 1 \quad\text{and}\quad \frac{TA\mathrm{e}^{-E/RT}}{b\Omega} \ll 1,$$

at least where $(1-\alpha)\alpha$ is not small (when the reaction is noticeably underway and not essentially finished).

With such a high frequency the cyclic contribution to the rate of heat absorption comes directly from the temperature-dependent factor and the oscillatory part of the concentration is unimportant: $\tilde{f}$ is in phase with $\tilde{T}$ and out of phase with $\mathrm{d}\tilde{T}/\mathrm{d}t$.

The first integral of (16),

$$\frac{HMT_1a_0}{C_Rb}\int_0^{\tau}\mathrm{e}^{(KT_1/bC_R)(s-\tau)}\,\bar{\alpha}g\,\mathrm{d}s,$$

can be approximated by $\frac{HMT_1a_0}{C_Rb}\times\frac{bC_R}{KT_1}g\bar{\alpha}(\tau)$, (using Watson's Lemma for instance, see [10] or [11], if $KT_1/bC_R \gg 1$. This last assumption is the same as the requirement that transients be negligible.

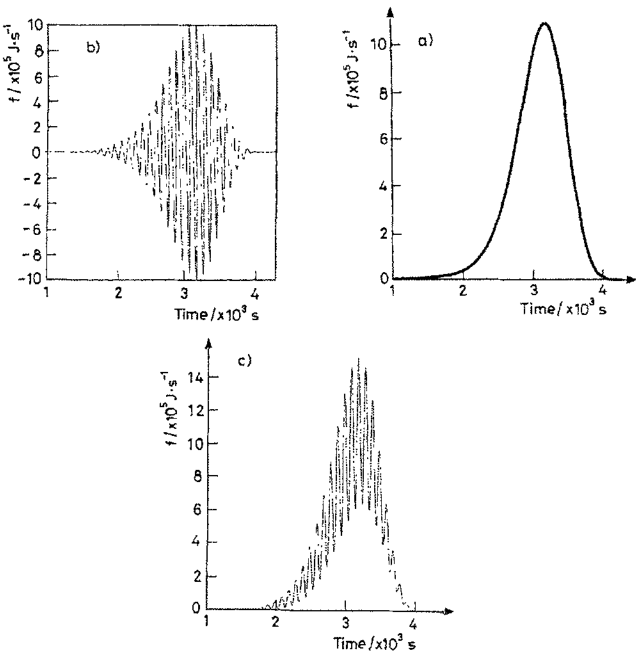

Fig. 1 The underlying (a), cyclic (b), and total (c) reaction rates

The second of the integral is approximately:

$$\frac{HBMT_1a_0}{C_Rb}\int_0^{\tau}e^{-(KT_1/bC_R)(s-\tau)}\,\bar{\alpha}g'\sin\Omega s\,\mathrm{d}s \cong \frac{HBMT_1a_0}{C_Rb}\times\frac{\bar{\alpha}g'}{(KT_1/bC_R)^2+\Omega^2}$$

$$\times\left(\frac{KT_1}{bC_R}\sin\Omega t-\Omega\cos\Omega\tau\right),$$

with the earlier assumptions, that $KT_1/bC_R \gg 1$ and $RT\Omega/E \gg 1$. Then

$$\Delta T \cong \frac{1}{K}(bC_s+HM\bar{\alpha}g)+\frac{B}{K^2+\omega^2C_R^2}\times$$

$$\left[(C_sC_R\omega^2+HMK\bar{\alpha}g')\sin\omega t+(KC_s\omega-\omega HMC_R\bar{\alpha}g')\cos\omega t\right] \qquad (21)$$

so that the underlying and cyclic measurements are, approximately,

$$\overline{C}_s = C_s\left(1 + \frac{HM\bar{a}g}{bC_s}\right),$$

$$\widetilde{C}_s = C_s\sqrt{1 + \left(\frac{HM\bar{a}g'}{\omega C_s}\right)^2},$$

according to (7) and (8) respectively. These can be rewritten in the more general forms

$$\overline{C}_s = C_s\left(1 + \frac{r}{bC_s}\right) \tag{22}$$

and

$$\widetilde{C}_s = C_s\sqrt{1 + \left(\frac{r'}{\omega C_s}\right)^2}, \tag{23}$$

where $r=HV\bar{a}g$ is the (underlying) rate of intake of heat by the reaction and $r' = \frac{\partial R}{\partial T} = HM\bar{a}g'$ (i.e. r' is a measure of sensitivity of r's dependence on temperature).

The two relative errors are

$$\frac{\text{rate of absorption of heat by the reaction}}{\text{ramp} \times \text{sample heat capacity}}$$

and the square of

$$\frac{\text{temperature derivative of heat absorption rate}}{\text{frequency} \times \text{sample heat capacity}}.$$

Note that the latter can be rapidly decreased by increasing the frequency of the modulation. The former is limited since the ramp cannot take very large values; for example, transients would not decay if b is not small compared to KT_1/C_R.

It should be noted that, at least to leading order, the underlying response is the same as that for conventional DSC.

For such an endothermic reaction, where it has been assumed that heat capacity stays constant (or nearly so), the two measured heat capacities both exhibit peaks, but of generally quite different shapes and positions of maxima. (Of course with an exothermic event the underlying measurement exhibits a dip although the cyclic one still has a peak.)

For the full Arrhenius expression, (12) the derivative is $g'(t)=(EA/RT^2)\exp(-E/RT)$. It follows that the shapes of the two curves are (for a first-order reaction)

$$\exp\left[-\frac{E}{R(T_0+bt)}-A\int_0^t e^{-E/R(T_0+bt_1)}\mathrm{d}t_1\right]$$

and

$$(T_0+bt)^{-2}\exp\left[-\frac{E}{R(T_0+bt)}-A\int_0^t e^{-E/R(T_0+bt_1)}\mathrm{d}t_1\right]$$

so the cyclic value takes it maximum somewhat before (corresponding to a lower temperature T_0+bt) that of the underlying.

Determination of the theoretical variation of the measured heat capacities is more straightforward if the activation energy is high. With $E/RT\gg1$ (at least where the reaction occurs) the Frank-Kamenetskii approximation is used and $Ae^{-E/RT}$ can be replaced $Ae^{-1/\varepsilon}e^{U}=A^*e^{U}$, where

$$\varepsilon=\frac{RT_a}{E}\ll 1, \tag{24}$$

T_a is a suitable typical temperature, say that when the reaction becomes perceptible or when the reaction rate is greatest, and U is a dimensionless (scaled) temperature given by

$$T=T_a(1+\varepsilon U).$$

With this simple exponential dependence upon temperature $g'\propto g$ so that now $\bar{C}_s$ and $\tilde{C}_s$ have peaks at the same time (and temperature) and they have quite similar graphs.

The formula for the underlying concentration, (14), becomes

$$\bar{a}=a_0\exp\left[-\frac{A^*\varepsilon T_a}{b}e^{(\bar{T}_s-T_a)/\varepsilon T_a}\right].$$

(Here $\bar{T}_s=T_0+bt$.) Following this,

$$r\cong A^*HMa_0\exp\left[\frac{\bar{T}_s-T_a}{\varepsilon T_a}-\frac{A^*\varepsilon T_a}{b}e^{(\bar{T}_s-T_a)/\varepsilon T_a}\right]$$

and

$$r'\cong\frac{A^*HMa_0}{\varepsilon T_a}\exp\left[\frac{\bar{T}_s-T_a}{\varepsilon T_a}-\frac{A^*\varepsilon T_a}{b}e^{(\bar{T}_s-T_a)/\varepsilon T_a}\right]$$

are proportional to each other and contribute to make an overall rate of heat absorption

$$f = r + Br'\sin\omega t$$

as shown (with exaggerated oscillatory part) in Fig. 2.

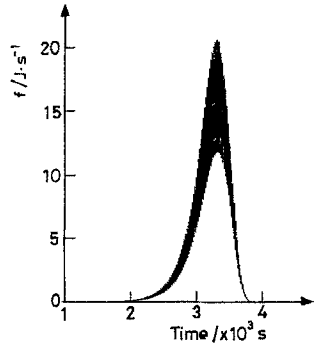

Fig. 2 Reaction rate with emphasized cyclic part for a first-order, high-activation-energy reaction

The theoretical underlying and cyclic values, $\bar{C}_s$ and $\tilde{C}_s$, taking T_o=270 K, b=0.05 K s^{-1}, ω=π/10 s^{-1}, B=0.3 K, C_s=7.5·10^{-3} J K^{-1}, K=10^{-2} W K^{-1}, C_R= 5·10^{-3} J K^{-1}; H=7.5·10^5 J kg^{-1}, E=1.5·10^5 J mol^{-1}, A=1.6·10^5 s^{-1} (one part sodium bicarbonate to ten parts alumina in a 10^{-5} kg sample) are plotted in Fig. 3(a) while experimental values are shown in Fig. 3(b).

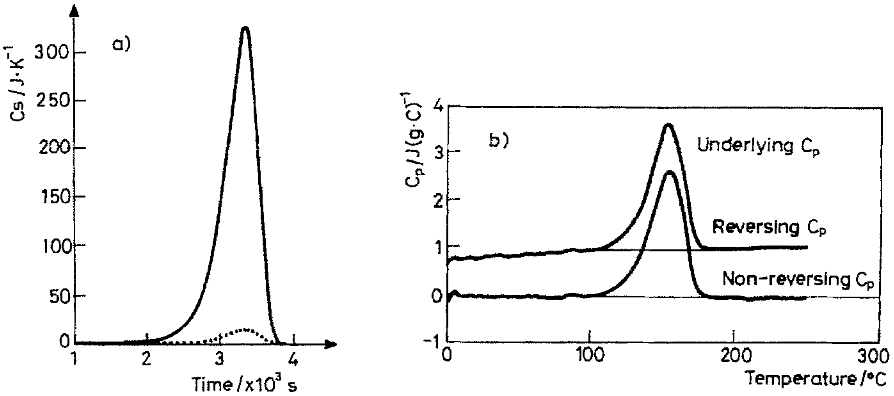

Fig. 3 Changes in measured values of heat capacity as functions of time for a first-order endothermic reaction with a high activation energy. In (a) simulated results are shown; the cyclic (broken and lower) curve has been scaled by a factor of 100 to make it more visible. In (b) experimental results are displayed (with *ω=20 s^{-1}*); the top curve (with peak) shows the underlying measurement. $\bar{C}_s$, the next curve (no peak) gives the cyclic measurement, $\tilde{C}_s$; the non-reversing signal is their difference and is the lower peaked curve

Figure 3 illustrates the advantage of using the modulation. The cyclic measurement, even without using the improvement noted in the following subsection, gives a reasonable estimate of the heat capacity (the maximum error being about 0.2%). Once C_s is determined its contribution can be subtracted from the underlying (conventional) measurement to find the reaction rate, or "nonreversing" component of the signal. (The term "nonreversing" applies to the effect of the irreversible reaction in contrast to the "reversing" part of the signal which, in this case, is simply due to the specific heat of the sample.)

The shapes of the curves are given by the form of r, effectively by $\exp(U-A^{+}e^{U})$, $(A^{+}=A^{*}\varepsilon T_a/b)$. After a shift of axis of U by $\ln A^{+}$ this is proportional to $\exp(U-e^{U})$ (Fig. 4). (Operational parameters and quantities such as activation energy simply affect the size so we omit the scales on Figs 4 and 5.)

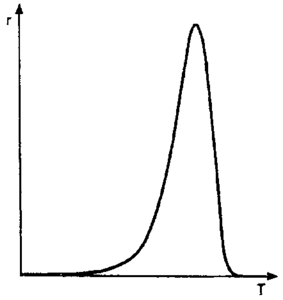

Fig. 4 Form of r and r', $\exp(U-e^{U})$, for a first-order endothermic reaction with a high activation energy

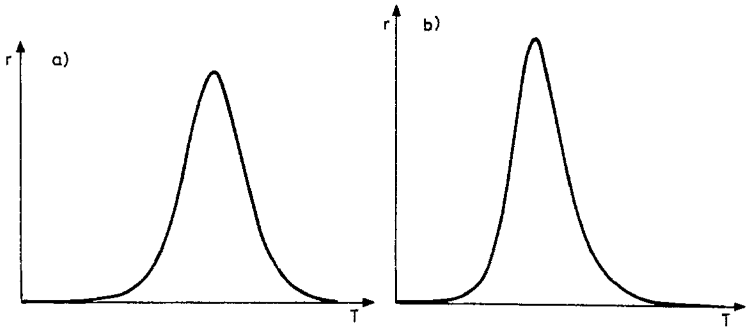

Fig. 5 Form of reaction rate for high-activation-energy reaction (a) 2nd-order reaction (b) 3rd-order reaction

The form of the graph, with a gradual increase $\cong(e^{U})$ and rapid decay (rather like $e^{-e^{U}}$ is characteristic of a first-order reaction. With a second-order reaction r and r' are proportional to $e^{U}/(1+A^{+}e^{U})^{2}$ (where $A^{+}=a_0A^{*}\varepsilon T_a/b$), with $U=(T-T_a)/\varepsilon T_a$ still being the normalized temperature. Again changing the temperature zero allows this function to be simplified, this time to $(e^{U/2}+e^{-U/2})^{-2}=1/4\mathrm{sech}^{2}U/2$, which is symmetric (Fig. 5(a)). For higher-order reactions the growth of r and r' is more rapid and the decay more gradual. For example, a third-order reaction has $r \propto e^U/(1+A^+e^U)^{3/2}$, or on shifting the temperature axis, $e^U/(1+e^U)^{3/2}$ (Fig. 5(b)).

A simpler model for a kinetic event might be given by taking the rate of heat intake to be purely a function of temperature, $f=f(T_s)$. Now supposing that f has a single peak near some "reaction temperature" T_c and decays to zero as $|T-T_c|$ gets large, then

$$\overline{C}_s \cong C_s + \frac{f}{b}$$

again has a single hump. Now

$$\tilde{C}_s \cong C_s\sqrt{1+\left(\frac{f'}{\omega C_s}\right)^2}$$

takes a very different form. It has a pair of maxima, corresponding to the greatest positive and negative values of f', and has a minimum with the true value C_s where f is largest, that is, where $\overline{C}_s$ achieves its maximum.

In practical terms the analysis given above means that in many cases it is possible to separate out the contribution to the heat flow which comes form the sample's heat capacity and that part which comes from the chemical reaction. We characterise the heat-capacity contribution as the reversing signal because it is clearly reversible. We prefer the terminology reversing rather than reversible because, as we shall see in Section 5.2, we can also separate out the contribution from the latent heat of crystallisation from that due to heat capacity and clearly crystallisation is a reversible process. Reversing means, in this context, rapidly reversible at the time and temperature that the measurement is made. As mentioned above, we can subtract this contribution from the total heat flow to find the nonreversing contribution. In the case of many chemical reactions these are irreversible and the meaning is clear. In other cases the chemical reaction might be in some way reversible but the non-reversing contribution will arise from the reaction not being reversible at the time and temperature of the measurement. For example an equivalent analysis to that given above would apply to the loss of volatiles such as moisture during a heating experiment. It may be possible to reabsorb the moisture by lowering the temperature and exposing it to the relevant vapour. However, the enthalpy associated with the loss of the volatile will be nonreversing as the measurement is made. In all of these cases, chemical reactions, crystallisations and loss of volatiles the rate at which they occur will be governed by some kinetic law, thus we also refer to these as kinetic or kinetically hindered processes [1–4]. When these occur at a measurable rate there will be peak in the nonreversing signal and also one in the out-of-phase (with dT/dt) cyclic signal and, therefore, in the phase lag. In many cases we have found [1–4] that this out-of-phase component is small and can be neglected, thus the heat capacity can be calculated from the amplitude of the cyclic signal alone. This is the "simple" deconvolution described in [1]. In other cases it might be desirable to use the phase lag to obtain a more accurate value for the sample heat capacity and this is described in the next section.

2.4 The use of the phase lag

The ability to linearize and neglect transients allows a simpler approach to be used. All quantities are regarded as being made up of an underlying and cyclic part (with no harmonics or subharmonics in the latter; [7] considers a case with higher harmonics present).

Thus for $T_s=T_o+bt+B\sin\omega t$, $da/dt=-ag(T_s)$, the reactive rate of heat absorption is approximately, with the assumed relative sizes of physical constants in §2.3,

$$f \cong HM\bar{a}g + BHM\bar{a}g'\sin\omega t$$

(using linearization and, because of high frequencies, retaining only the dominant cyclic part)

$$= r + Br'\sin\omega t = \text{underlying part} + \text{cyclic part;}$$

as before $\bar{a}$ is given by $\bar{a}=a_o\exp[-\int_o^t g(t_o+bt_1)dt_1]$ (still taking the reaction to be first-order), and g and g' are evaluated at $T=T_o+bt$.

Equation (5) can then be written as

$$C_R\frac{d\Delta T}{dt} + K\Delta T = (C_sb + r) + B(\omega C_s\cos\omega t + r'\sin\omega t).$$

The solution is written as $\Delta T=\overline{\Delta T}$ (underlying part = equivalent response in conventional DSC) $+\widetilde{\Delta T}$ (cyclic part). These two parts are given (approximately) by

$$\overline{\Delta T} = \frac{1}{K}(C_sb + r)$$

(as before) and

$$C_R\frac{d\widetilde{\Delta T}}{dt} + K\widetilde{\Delta T} = B\mathrm{Re}\left\{\omega C_s e^{i\omega t} - ir'e^{i\omega t}\right\}$$

$$= \omega B\mathrm{Re}\left\{\left(C_s - \frac{ir'}{\omega}\right)e^{i\omega t}\right\}. \qquad (25)$$

(The cyclic parts of the sample temperature and its rate of change are $B\mathrm{Im}\{e^{\mathrm{i}\omega \mathrm{b}}\}$ and $B\omega\mathrm{Re}\{\mathrm{e}^{\mathrm{i}\omega \mathrm{b}}\}$ respectively.)

This can be contrasted with the equivalent equation for an inert sample, $C_\mathrm{R}\mathrm{d}\widetilde{\Delta T}/\mathrm{d}t+K\widetilde{\Delta T}=\omega B\mathrm{Re}\{C_\mathrm{s}\mathrm{e}^{\mathrm{i}\omega t}\}$. The real heat capacity is replaced by the complex heat capacity $C_\mathrm{s}-\mathrm{i}r'/\omega$. Employing this quantity, which was introduced in [4], does not alter the fundamental theory but it enables calculations involved in the analysis to be carried out more easily. (Complex heat capacities also appear in [8, 12].)

In solving (25) we can again, because of the high frequency, neglect changes in r' and C_s (which happen slowly compared with the variation of $\mathrm{e}^{\mathrm{i}\omega t}$) as well as the transients to give

$$\begin{aligned}\widetilde{\Delta T}&=\omega B\mathrm{Re}\left\{\frac{C_\mathrm{s}-\mathrm{i}r'/\omega}{K+\mathrm{i}\omega C_\mathrm{R}}\mathrm{e}^{\mathrm{i}\omega t}\right\}\\&=\omega BC_\mathrm{s}\sqrt{\frac{1+(r'/\omega C_\mathrm{s})^2}{K^2+\omega^2C_\mathrm{R}^2}}\,\mathrm{Re}\{\mathrm{e}^{\mathrm{i}(\omega t-\varphi)}\}\end{aligned}\tag{26}$$

where φ is the phase lag,

$$\varphi=\tan^{-1}\frac{\omega C_\mathrm{R}}{K}+\tan^{-1}\frac{r'}{\omega C_\mathrm{s}}.$$

The cyclic (amplitude) measurement of heat capacity is again seen to be

$$\begin{aligned}\widetilde{C}_\mathrm{s}&=\frac{\sqrt{K^2+\omega^2C_\mathrm{R}^2}\times\text{Amplitude of temperature difference}}{\text{Amplitude of rate of change of sample temperature}}\\&=C_\mathrm{s}\sqrt{1+\left(\frac{r'}{\omega C_\mathrm{s}}\right)^2}\end{aligned}$$

since the amplitude of $\mathrm{d}T_\mathrm{s}/\mathrm{d}t$ is ωB and the calibration factor is $\sqrt{K^2+\omega^2C_\mathrm{R}^2}=K\times\sqrt{1+(\omega C_\mathrm{R}/K)^2}=$ heat transfer coefficient × correction factor.

It can be observed that the phase lag is made up of two parts. The first, $\varphi_\mathrm{b}=\tan^{-1}(\omega C_\mathrm{R}/K)$ is independent of the sample and can be found either by calibration or interpolation from places where no reaction occurs; this is the "baseline" phase lag [1]. The second part, the corrected phase lag $(\varphi-\varphi_\mathrm{b})$, is $\varphi_\mathrm{c}=\tan^{-1}(r'/\omega C_\mathrm{s})$ and depends upon the reaction rate as well as the sample's heat capacity; $\varphi=\varphi_\mathrm{b}$ and $\varphi_\mathrm{c}=0$ if there is no significant kinetic event.

Once φ_c has been determined the heat capacity can be obtained more accurately since $\sqrt{1+(r'/\omega C_\mathrm{s})^2}=\sec\varphi_\mathrm{c}$:

$$C_s = \tilde{C}_s\cos\varphi_c = \frac{|\Delta\tilde{T}|}{B\omega}\sqrt{K^2 + \omega^2 C_R^2}\,\cos\varphi_c.$$

The reaction rate r can then be found from

$$r = b(\overline{C}_s - C_s) = K\Delta T - bC_s.$$

Thus the out-of-phase component is the derivative of the heat flow arising from the chemical reaction with respect to temperature multiplied by the amplitude of the temperature modulation. The phase lag which arises from the instrument, see Section 2.2, is corrected for by interpolation of the baseline from either side of the phase lag peak. This is the "complete" deconvolution described in [1]. An alternative would be to take the baseline from an experiment with an inert sample. As mentioned above the out-of-phase kinetic component is often small and can be neglected during chemical reactions, loss of volatiles, crystallisations and glass transitions, [1–3]; however, the further refinement of using the phase angle can be applied if desired [1]. In the case of the glass transtion the separation of the signal into reversing and nonreversing components is less straightforward to interpret than the other kinetic process considered above, due to the frequency dependence of the sample heat capacity in the region of the glass transition. However there is a parallel between the enthalpy loss on annealing and the other kinetic processes considered here. We shall provide a detailed analysis of the glass transition in another publication [13].

The phase shift during melting is generally large, [1–3]. We present the first part of our analysis of melting behaviour below, Section 5, but this does not account for the phase shift which will be the subject of a future article.

2.5 Non-ideal calorimeters: Thermal resistance and bias

Apart from requirements about the sizes of frequency and amplitude of oscillation two key assumptions above were that the temperatures measured by the thermocouples are precisely those of the pans and the device is perfectly symmetric. This subsection discusses the consequences of one or the other of these assumptions (but not both together) being violated.

Should there be significant thermal resistances between the pans and thermocouples the measured temperature $T_{SM}(=T_0+bt+B\sin\omega t)$ and T_{RM} are no longer exactly those of the sample and reference. To keep the calculations as simple as possible while investigating the consequences of such an occurrence the working is limited to a model where the heat transfer to and from a pan is only from and to the block; there is no direct thermal connection between the pans. The measured temperature for a pan is a linear combination of the true temperature and that of the block (corresponding to the thermocouple being at a point somewhere between the two).

Starting with the simple case of an inert sample heat balance again gives

$$(C_R + C_s)\frac{dT_s}{dt} = K(T_F - T_s),$$

$$C_R\frac{dT_s}{dt} = K(T_F - T_R),$$

with the measured temperatures being

$$T_{SM} = T_o + bt + B\sin\omega t = (1 - \eta)T_s + \varepsilon T_F,$$

$$T_{RM} = (1 - \eta)T_R + \varepsilon T_F.$$

Here $0<\eta<1$ is a measure of the thermal resistance or error; it should be small.

Taking the same sort of approach as in the previous subsection each temperature T_j (j=S, F, R, SM or RM) is written as

$$T_j = T_{oj} + bt + \mathrm{Im}\{B_j e^{i\omega t}\}.$$

The underlying parts ($\bar{T}_{oj}=T_{oj}+bt$) satisfy

$$(C_R + C_s)b = K(T_{OF} - T_{OS}), \quad C_R b = K(T_{OF} - T_{OR}),$$

$$T_O = T_{OSM} = (1 - \eta)T_{OS} + \eta T_{OF},$$

and

$$T_{ORM} = (1 - \eta)T_{OR} + \eta T_{OF},$$

so

$$T_{OS} = T_O - \frac{\eta(C_R + C_s)b}{K},$$

$$T_{ORM} = T_O - \frac{(1 - \eta)C_s b}{K},$$

and

$$\overline{\Delta T}_M = \bar{T}_{RM} - \bar{T}_{SM} = \frac{b(1 - \eta)C_s}{K}.$$

The method of using the underlying measurements is essentially the same as before, the only difference being that K has been replaced by $K/(1-\eta)$.

Turning to the cyclic contribution,

$$i\omega B_s = (C_R + C_s) = K(B_F - B_s),$$

$$i\omega B_s C_R = K(B_F - B_R),$$

$$B = (1 - \eta)B_s + \eta B_F,$$

and

$$B_{RM} = (1 - \eta)B_R + \eta B_F,$$

which give

$$B_F = \frac{K + i\omega(C_R + C_s)}{K + i\eta\omega(C_R + C_s)}B,$$

$$B_{RM} = \left(\frac{K + i\eta\omega C_R}{K + i\omega C_R}\right)\left(\frac{K + i\omega(C_R + C_s)}{K + i\eta\omega(C_R + C_s)}\right)B,$$

and

$$\Delta B_M = B_{RM} - B_{SM} = B_{RM} - B = \frac{i\omega K C_s(1 - \eta)B}{(K + i\omega C_R)[K + i\eta\omega(C_R + C_s)]}.$$

The cyclic part of the (measured) temperature difference is

$$\begin{aligned}\tilde{\Delta}T_M &= \omega K(1 - \eta)C_s B\,\mathrm{Re}\left\{\frac{e^{i\omega t}}{(K + i\omega C_R)[K + i\eta\omega(C_R + C_s)]}\right\}\\ &= \frac{(1 - \eta)B\omega C_s}{\sqrt{1 + (\omega C_R/K)^2}\sqrt{1 + [\eta\omega(C_R + C_s)/K]^2}}\cos(\omega t - \varphi).\end{aligned}\tag{27}$$

A possible difficulty is now evident. If C_s is comparable with (or larger than) the bigger of C_R and $K/\eta\omega$ (as might happen with a very large sample and very poor thermal contact between the thermocouples and pans), then the amplitude $|\tilde{\Delta}T_M|$ depends nonlinearly upon the heat capacity C_s. On the other hand if C_s is small then the calibration factor relating the ratio of the amplitudes of the temperature difference and of the rate of temperature change is

$$K\frac{\sqrt{1 + (\omega C_R/K)^2}\sqrt{1 + (\eta\omega C_R/K)^2}}{1 - \eta}.$$

This reduces to the factor appropriate for good thermal conduct when η vanishes. The phase lag φ now also depends upon C_s:

$$\varphi = \varphi_b \equiv \tan^{-1}\frac{\omega C_R}{K} + \tan^{-1}\frac{\eta\omega(C_R + C_s)}{K}.$$

The effect of heat intake by a reaction can be allowed for using the complex-heat-capacity approach. The underlying temperature difference is

$$\overline{\Delta T_{\mathrm{M}}} = \frac{1-\eta}{K}(bC_s + r)$$

so $\overline{C_m}=C_s+r/b$ as previously.

The cyclic part is

$$\widetilde{\Delta T}_{\mathrm{M}} = K(1-\eta)B\,\mathrm{Re}\left\{\frac{(\omega C_s - ir')e^{i\omega t}}{(K+i\omega C_{\mathrm{R}})(K+\eta[i\omega(C_{\mathrm{R}}+C_s)+r'])}\right\}$$

$$= K(1-\eta)B\omega C_s\sqrt{\frac{1+(r'/\omega C_s)^2}{(K^2+\omega^2C_{\mathrm{R}}^2)[(K+\eta r')^2+(\eta\omega(C_{\mathrm{R}}+C_s))^2]}}\cos(\omega t-\varphi)$$

with

$$\varphi = \tan^{-1}\frac{\omega C_{\mathrm{R}}}{K} + \tan^{-1}\frac{r'}{\omega C_s} + \tan^{-1}\frac{\eta\omega(C_{\mathrm{R}}+C_s)}{K+r'\eta}.$$

Supposing that C_s is small enough for the inert situation to be linear the measurement of C_s based upon the amplitude of $\Delta\widetilde{T}_{\mathrm{M}}$ is

$$\widetilde{C}_{\mathrm{S}} = C_s\sqrt{\frac{[1+(r'/\omega C_s)^2][K^2+(\eta\omega C_{\mathrm{R}})^2]}{(K+\eta r')^2+[\eta\omega(C_{\mathrm{R}}+C_s)^2]}}$$

$$\cong C_s\sqrt{\frac{[1+(r'/\omega C_s)^2][K^2+(\eta\omega C_{\mathrm{R}})^2]}{(K+\eta r')^2+(\eta\omega C_{\mathrm{R}})^2}}$$

unless C_s is only small in comparison with $K/\eta\omega$ and $\eta r'\cong -K$.

The corrected phase lag also depends in a more complicated fashion on the reaction rate and heat capacity:

$$\varphi_c = \tan^{-1}\frac{r'}{\omega C_s} + \left[\tan^{-1}\frac{\eta\omega(C_{\mathrm{R}}+C_s)}{K+\eta r'} - \tan^{-1}\frac{\eta\omega(C_{\mathrm{R}}+C_s)}{K}\right].$$

Even for cases where $C_s \ll C_{\mathrm{R}}$ (a "small sample"), so that when they are inert there is linearity, the corrected phase lag

$$\cong \tan^{-1}\frac{r'}{\omega C_s} + \left[\tan^{-1}\frac{\varepsilon\omega C_{\mathrm{R}}}{K+\eta r'} - \tan^{-1}\frac{\eta\omega C_{\mathrm{R}}}{K}\right]$$

and can depend upon the constituents of the calorimeter through K, C_{R}, and η.

In practice nonlinear dependence of $\Delta\tilde{T}$ upon C_s and variation of φ_c with change of purge gas (N_2 or He) are not significant: there is good thermal contact and the terms in η can generally be neglected. Experimental results with a variety of sample sizes under both helium and nitrogen, a change that would greatly affect the quality of the thermal contact between the crucible and the thermocouple sensors, give results that are within the range of normal experimental error for heat capacity determinations, (Fig. 6), reasonable results can be obtained under both gases. This implies that problems of poor thermal conduction do not introduce gross errors. We have found that the results under helium are more repeatable and seem completely unaffected by sample size whereas there is a measurable trend under nitrogen. This suggests that for best results helium should be used as the purge gas.

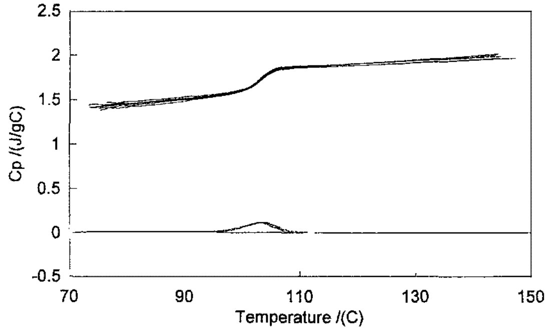

Fig. 6 Experimental results using helium and nitrogen. $C'=\tilde{C}_s\cos\varphi_c$ (upper curves) and $C''=\tilde{C}_s\sin\varphi_c$ (lower curves) are the real and imaginary parts of the (cyclic) measured heat capacity. Around the transition the variation between experiments is within experimental error for the technique. Samples are 5, 10, 20 mg of polystyrene under N_2 and He purges

(If thermal contact were poor there would be additional difficulty due to reaction rate depending on T_s, not on T_{SM}:

$$a = a_0\exp\left[-\int_0^t g(\bar{T}_s)\,\mathrm{d}t\right] \neq a_0\exp\left[-\int_0^t g(T_o + bt)\,\mathrm{d}t\right]$$

and $r=ag(T_s)$.)

The same type of approach can be taken for a biased calorimeter. Again supposing that each pan is in direct thermal contact with the block, the heat-transfer coefficient for the sample is now λ times that for the reference:

$$(C_R + C_s)\frac{\mathrm{d}T_s}{\mathrm{d}t} = \lambda K(T_F - R_s)$$

and

$$C_R\frac{dT_R}{dt} = K(T_F - T_R)$$

(with no kinetic event). Once again $T_s = T_0 + bt + B\sin\omega t$.

The temperature difference $T_R - T_s$ now satisfies the differential equation

$$C_R + \frac{d\Delta T}{dt} + K\Delta T = \left[\frac{C_s}{\lambda} + C_R\left(\frac{1}{\lambda} - 1\right)\right]\frac{dT_s}{dt}$$

$$= \frac{1}{\lambda}(C_s + (1 - \lambda)C_R)(b + B\omega\cos\omega t).$$

The underlying and cyclic parts (as usual ΔT may be taken to be nearly periodic) are

$$\overline{\Delta T} = \frac{b}{K\lambda}[C_s + (1 - \lambda)C_R]$$

and

$$\Delta\tilde{T} = \frac{[C_s + (1 - \lambda)C_R]}{\lambda}B\omega\mathrm{Re}\left\{\frac{e^{i\omega t}}{K + i\omega C_R}\right\}$$

$$= \frac{[C_s + (1 - \lambda)C_R]B\omega}{\lambda\sqrt{K^2 + \omega^2 C_R^2}}\cos(\omega t - \varphi).$$

Calibration can be used to determine the offset term $(1-\lambda)C_R$ (or equivalently $(1-\lambda)\ C_R/K\lambda$) as well as the calibrating factors $K\lambda$ and $\lambda\sqrt{K^2 + \omega^2 C_R^2}$, so then

$$\overline{C_s} = \frac{K\lambda\overline{\Delta T}}{b} + (\lambda - 1)C_R$$

and

$$\tilde{C_s} = \frac{\lambda\sqrt{K^2 + \omega C_R^2}\,|\Delta\tilde{T}|}{B\omega} + (\lambda - 1)C_R$$

are the two measurements of heat capacity. (The amplitude of $\tilde{\Delta T}$ is still denoted by $|\tilde{\Delta T}|$). Of course it is now necessary to carry out a second calibrating run because of the extra unknown due to the bias.

Once again the effect of a chemical reaction is easily included.

$$\overline{\Delta T} = \frac{1}{K\lambda}[bC_s + r + b(1 - \lambda)C_R]$$

and

$$\tilde{\Delta}T = \frac{B\omega}{\lambda}\mathrm{Re}\left\{\frac{C_s - \mathrm{i}r'/\omega + (1-\lambda)C_R}{K + \mathrm{i}\omega C_R}\,\mathrm{e}^{\mathrm{i}\omega t}\right\}$$

lead to estimates $\overline{C}_s = C_s + r/b$ and $\tilde{C}_s = \sqrt{[C_s + (1-\lambda)C_R]^2 + (r'\omega)^2} + (\lambda - 1)C_R$ for the heat capacity. The corrected phase lag in this case is

$$\varphi_c = \tan^{-1}\frac{r'}{\omega[C_s + (1-\lambda)C_R]}$$

and an improved value for C_s is given by

$$\frac{\lambda\sqrt{K^2 + \omega^2 C_R^2}}{B\omega}\,|\tilde{\Delta}T|\,\cos\varphi_c + (\lambda - 1)C_R.$$

3. Processing the measurements

One aspect of the experiment that is still to be discussed is the identification of the underlying and cyclic parts of the signal.

For example, according to Eq. (21) the temperature difference ΔT is of the approximate form

$$\Delta T(t) = F(t) + B[G(t)\sin\omega t + I(t)\cos\omega t].$$

The terms $G\sin\omega t$ and $I\cos\omega t$ account for all the oscillations: F, G, I are smoothly varying (and contain no terms like $\sin\omega t$ or $\cos\omega t$).

Assuming that such a difference is measured exactly the underlying signal is found by taking some average. For an ideal case this means taking an integral. (In practice values at discrete times will be summed). Using one period of the modulation the measured underlying value is

$$\overline{\Delta T_M}(t) = F_M(t) = \frac{\omega}{2\pi}\int_{t-\pi/\omega}^{t+\pi/\omega}\Delta T(\tau)\mathrm{d}\tau$$

$$= \frac{1}{2\pi}\int_{-\pi}^{\pi}\left\{F(t) + \frac{s}{\omega}\frac{\mathrm{d}F}{\mathrm{d}t}(t) + \frac{s^2}{2\omega^2}\frac{\mathrm{d}^2F}{\mathrm{d}t^2}(t) + \ldots\right.$$

$$+ B\left[G(t) + \frac{s}{\omega}\frac{\mathrm{d}G}{\mathrm{d}t}(t) + \frac{s^2}{2\omega^2}\frac{\mathrm{d}^2G}{\mathrm{d}t^2}(t) + \ldots\right]$$

$$\times(\sin\omega t\cos s + \cos\omega t\sin s)$$

$$+B\left[I(t)+\frac{s}{\omega}\frac{\mathrm{d}I}{\mathrm{d}t}(t)+\frac{s^2}{2\omega^2}\frac{\mathrm{d}^2I}{\mathrm{d}t^2}(t)+\ldots\right]$$

$$\times(\cos\omega t\cos s-\sin\omega t\sin s)\}\,\mathrm{d}s.$$

(This is given by writing $\tau=t+s/\omega$ and expanding F, G and I about t.)

The extracted underlying signal is not precisely F but rather

$$\overline{\Delta T}=F_{\mathrm{M}}\cong F+\frac{\pi^2}{6}\omega^{-2}\frac{\mathrm{d}^2F}{\mathrm{d}t^2}+\ldots+B\Big[\omega^{-1}\frac{\mathrm{d}G}{\mathrm{d}t}\cos\omega t-\omega^{-2}\frac{\mathrm{d}^2G}{\mathrm{d}t^2}\sin\omega t\ldots$$

$$-\omega^{-1}\frac{\mathrm{d}I}{\mathrm{d}t}\sin\omega t-\omega^{-2}\frac{\mathrm{d}^2I}{\mathrm{d}t^2}\cos\omega t\ldots.\Big]\tag{28}$$

The first Fourier coefficients can be determined by either first finding

$$\Delta T_{\mathrm{s}}(t)=\frac{\omega}{\pi}\int_{t-\pi/\omega}^{t+\pi/\omega}\Delta T(\tau)\sin\omega t\,\mathrm{d}\tau$$

and

$$\Delta T_{\mathrm{c}}(t)=\frac{\omega}{\pi}\int_{t-\pi/\omega}^{t+\pi/\omega}\Delta T(\tau)\cos\omega t\,\mathrm{d}\tau$$

and then taking averages over a cycle,

$$\overline{\Delta T_{\mathrm{s}}}(t)=B\overline{G}_{\mathrm{m}}(t)\equiv\frac{\omega}{2\pi}\int_{t-\pi/\omega}^{t+\pi/\omega}\Delta T_{\mathrm{s}}(\tau)\,\mathrm{d}\tau$$

and

$$\Delta\overline{T}_{\mathrm{c}}(t)=BI_{\mathrm{M}}(t)\equiv\frac{\omega}{2\pi}\int_{t-\pi/\omega}^{t+\pi/\omega}\Delta T_{\mathrm{c}}(\tau)\,\mathrm{d}\tau,$$

or alternatively calculating the Fourier coefficients of the difference between ΔT and its "mean"

$$\Delta\tilde{T}_{\mathrm{s}}(t)=B\tilde{G}_{\mathrm{m}}(t)\equiv\frac{\omega}{\pi}\int_{t-\pi/\omega}^{t+\pi/\omega}[\Delta T(\tau)-\Delta\overline{T}_{\mathrm{M}}(\tau)]\sin\omega t\,\mathrm{d}\tau$$

and

$$\Delta\tilde{T}_{\mathrm{c}}\ (t) = BI_{\mathrm{M}}(t) \equiv \frac{\omega}{\pi}\int\limits_{t-\pi/\omega}^{t+\pi/\omega}[\Delta T(\tau) - \Delta\bar{T}_{\mathrm{M}}(\tau)]\cos\omega t\mathrm{d}\tau.$$

For "large" values of ω these again approximate values of BG and BI but the two methods do give slightly different answers. The former results in

$$\overline{\Delta T_{\mathrm{s}}} = B\bar{G}_{\mathrm{M}} \cong -\frac{2}{\omega^2}\frac{\mathrm{d}^2F}{\mathrm{d}t^2}\sin\omega t + \ldots + B\left(G + \frac{\pi^2}{3\omega^2}\frac{\mathrm{d}^2G}{\mathrm{d}t^2} + \ldots\right)$$
$$+\frac{B}{4\omega^2}\left(\frac{\mathrm{d}^2G}{\mathrm{d}t^2}\cos2\omega t - \frac{\mathrm{d}^2I}{\mathrm{d}t^2}\sin2\omega t + \ldots\right) \tag{29}$$

and

$$\Delta\bar{T}_{\mathrm{c}} = B\bar{I}_{\mathrm{M}} \cong -\frac{2}{\omega}\frac{\mathrm{d}^2F}{\mathrm{d}t^2}\cos\omega t + \ldots + B\left(I + \frac{\pi}{3}\frac{\mathrm{d}^2I}{\mathrm{d}t^2} + \ldots\right)$$
$$-\frac{B}{4\omega^2}\left(\frac{\mathrm{d}^2I}{\mathrm{d}t^2}\cos2\omega t + \frac{\mathrm{d}^2G}{\mathrm{d}t^2}\sin2\omega t + \ldots\right). \tag{30}$$

On dividing by the amplitude B of the sample's temperature oscillation the "measured" values take the form

$$\bar{G}_{\mathrm{M}} = G + \frac{\pi^2}{3\omega^2}\frac{\mathrm{d}^2G}{\mathrm{d}t^2} + \ldots + \text{oscillatory terms of" size}\frac{1}{B\omega^2}\text{" or smaller.}$$

This indicates that the error can be large if B is too small compared with ω. However, since the relevant terms are oscillatory, further averaging e.g.

$$\bar{\bar{G}}_{\mathrm{M}} = \int\limits_{t-\pi/\omega}^{t+\pi/\omega}\bar{G}_{\mathrm{M}}(\tau)\mathrm{d}\tau$$

can be used to reduce their size. (Of course too much smoothing might be undesirable and it certainly fails to eliminate systematic error terms such as $(\pi^2/3\omega^2)(\mathrm{d}^2G/\mathrm{d}t^2)$). It is clear that if the calorimeter and sample have constant physical properties the derivatives of F, G and I all vanish and these errors disappear.

The significance of the errors is illustrated by the example of a sample whose heat capacity depends upon temperature: $C_{\mathrm{s}}=C(T)$. Using the simple ODE model of Section 2,

$$C_{\mathrm{R}}\frac{\mathrm{d}\Delta T}{\mathrm{d}t} + K\Delta T = (b + B\omega\cos\omega t)C_{\mathrm{s}},$$

where now linearization gives

$$C_s = C(T_0 + bt + B\sin\omega t) = C + C'B\sin\omega t + \dots,$$

where, the C, $C'=\mathrm{d}C/\mathrm{d}T$ are evaluated at $T=\overline{T}_s+T_0+bt$.

The temperature difference then satisfies

$$C_R\frac{\mathrm{d}\Delta T}{\mathrm{d}t} + K\Delta T \cong bC + B(\omega C\cos\omega t + bC'\sin\omega t) \quad (+\text{ terms in } B^2, B^3, \dots)$$

$$= bC + B\mathrm{Re}\{(\omega C - \mathrm{i}bC')\mathrm{e}^{\mathrm{i}\omega t}\}.$$

The leading terms in an approximate solution of ΔT for ω and K large can be found either by using Laplace's method or the method of multiple scales, again see [10] or [11]. For the latter method, a change of time variable, $t = \tau/\omega$, gives

$$\psi\frac{\mathrm{d}\Delta T}{\mathrm{d}\tau} + \Delta T = \frac{b}{K}C + \frac{B\omega}{K}\mathrm{Re}\left\{\left(C - \frac{\mathrm{i}b}{\omega}C'\right)\mathrm{e}^{\mathrm{i}\tau}\right\}$$

where $\psi=\omega C_R/K$. The heat capacity C is taken to vary over a much slower time scale, $C=D(\sigma)$ with $\sigma=\delta t$ for some very small δ. Then

$$C' = \frac{\mathrm{d}C}{\mathrm{d}T} = \frac{1}{b}\frac{\mathrm{d}D}{\mathrm{d}t} = \frac{\omega}{b}\frac{\mathrm{d}D}{\mathrm{d}\tau} = \frac{\delta\omega}{b}\frac{\mathrm{d}D}{\mathrm{d}\sigma} = \frac{\delta\omega}{b}D'.$$

The oscillatory nature and slower drift of ΔT are taken into account by supposing that ΔT depends upon both τ and δ in which case

$$\frac{\mathrm{d}\Delta T}{\mathrm{d}\tau} = \frac{\partial\Delta T}{\partial\tau} + \delta\frac{\partial\Delta T}{\partial\sigma}$$

and the differential equation becomes

$$\psi\frac{\partial\Delta T}{\partial\tau} + \Delta T + \delta\psi\frac{\partial T}{\partial\sigma} = \frac{b}{K}D + \frac{\omega B}{K}\mathrm{Re}\{(D - \mathrm{i}\delta D')\mathrm{e}^{\mathrm{i}\tau}\}.$$

The solution is found as a series, $\Delta T \cong \Delta T_0 + \delta\Delta T_1 + \delta^2\Delta T_2 + \dots$, with the individual terms obtained on comparing coefficients of successive powers of δ:

$$\Delta T_0 = \frac{bD}{K} + \frac{\omega B}{K}\mathrm{Re}\left\{\frac{D}{(1+\mathrm{i}\psi)}\mathrm{e}^{\mathrm{i}\tau}\right\};$$

$$\Delta T_1 = -\frac{\psi bD'}{K} - \frac{\omega B}{K}\mathrm{Re}\left\{\frac{\mathrm{i}D'}{(1+\mathrm{i}\psi)^2}\mathrm{e}^{\mathrm{i}\tau}\right\};$$

$$\Delta T_2 = \frac{\psi^2 bD''}{K} - \frac{\omega B}{K}\mathrm{Re}\left\{\frac{\mathrm{i}\psi D''}{(1+\mathrm{i}\psi)^3}\mathrm{e}^{\mathrm{i}\tau}\right\}.$$

Combining these, returning to the original time t, and again using relations between derivatives (so $\psi\delta\ \mathrm{d}/\mathrm{d}\sigma = bC_\mathrm{R}/K\ \mathrm{d}/\mathrm{d}T$) yields

$$\Delta T \cong \frac{b}{K}C - \frac{b^2C_\mathrm{R}}{K^2}C' + \frac{b^3C_\mathrm{R}^2}{K^3}C'' \pm \ldots$$

$$+\ \omega B\mathrm{Re}\left\{\left[\frac{C}{(K+\mathrm{i}\omega C_\mathrm{R})} - \frac{\mathrm{i}KbC'}{\omega(K+\mathrm{i}\omega C_\mathrm{R})^2} + \frac{\mathrm{i}b^2KC_\mathrm{R}C''}{\omega(K+\mathrm{i}\omega C_\mathrm{R})^3} + \ldots\right]\mathrm{e}^{\mathrm{i}\omega t}\right\}.$$

(Still neglecting the nonlinear terms in A^2 etc.) Then

$$F(t) = \frac{b}{K}\left[C - \frac{bC_\mathrm{R}}{K}C' + \left(\frac{bC_\mathrm{R}}{K}\right)^2 C'' \pm \ldots\right],$$

$$G(t) = \frac{\omega^2C_\mathrm{R}C}{K^2+\omega^2C_\mathrm{R}^2} + \frac{Kb(K^2-\omega^2C_\mathrm{R}^2)C'}{(K^2+\omega^2C_\mathrm{R}^2)^2} + \frac{K^2b^2C_\mathrm{R}(3\omega^2C_\mathrm{R}^2-K^2)C''}{(K^2+\omega^2C_\mathrm{R}^2)^3}\ \ldots,$$

and

$$I(t) = \frac{\omega KC}{K^2+\omega^2C_\mathrm{R}^2} - \frac{2\omega bK^2C_\mathrm{R}C'}{(K^2+\omega^2C_\mathrm{R}^2)^2} + \frac{\omega b^2C_\mathrm{R}^2K(3K^2-\omega^2C_\mathrm{R}^2)C''}{(K^2+\omega^2C_\mathrm{R}^2)^3}\ \ldots.$$

The expansions appear in this form on thinking of K and ωC_R as having similar sizes and C being slowly varying (or the frequency as being large) so that

$$1 \gg \left(\frac{b}{\omega}\right)\frac{C'}{C} \gg \left(\frac{b}{\omega}\right)^2\frac{C''}{C} \gg \ldots,$$

i.e. quantities change by relatively small amounts as underlying temperature increases during one period. The expressions can be thought of as representing the true underlying, sine, and cosine components of ΔT.

These can be substituted into (28), (29) and (30) to give the measured components:

$$\overline{F}_\mathrm{M} = \overline{\Delta}T_\mathrm{M} = \frac{b}{K}\left[C - \frac{bC}{K}C' + \left(\frac{bC_\mathrm{R}}{K}\right)^2 C'' \pm \ldots + \frac{\pi^2}{6}\left(\frac{b}{\omega}\right)^2 C'' + \ldots\right]$$

$$+ \frac{BbC'}{K^2+\omega^2C_\mathrm{R}^2}(\omega C_\mathrm{R}\cos\omega t - K\sin\omega t)\ \ldots;$$

$$\overline{G}_\mathrm{M} = -\frac{2b^3C''}{BK\omega^2}\sin\omega t + \ldots + \frac{\omega^2C_\mathrm{R}C}{K^2+\omega^2C_\mathrm{R}^2} + \frac{bK(K^2-\omega^2C_\mathrm{R}^2)C'}{(K^2+\omega^2C_\mathrm{R}^2)^2}$$

$$+\left[\frac{b^2C_RK^2(3\omega^2C_R^2-K^2)}{(K^2+\omega^2C_R^2)^3}+\frac{\pi^2b^2C_R}{3(K^2+\omega^2C_R^2)}\right]C''+\ldots$$

$$+\frac{b^2C''}{4\omega(K^2+\omega^2C_R^2)}(\omega C_R\cos 2\omega t-K\sin 2\omega t)\ \ldots\ ;$$

$$I_M=-\frac{2b^3C''}{BK\omega^2}\cos\omega t+\ldots+\frac{\omega KC}{K^2+\omega^2C_R^2}-\frac{2\omega bK^2C_RC'}{(K^2+\omega^2C_R^2)^2}$$

$$+\left[\frac{\omega b^2KC_R^2(3K^2-\omega^2C_R^2)}{(K^2+\omega^2C_R^2)^3}+\frac{\pi^2b^2K}{3\omega(K^2+\omega^2C_R^2)}\right]C''+\ldots$$

$$-\frac{b^2C''}{4\omega(K^2+\omega^2C_R^2)}(K\cos 2\omega t+\omega C_R\sin 2\omega t)\ \ldots\ .$$

It follows that the underlying measurement is

$$\overline{C}=C-\left(\frac{bC_R}{K}\right)C'+\left[\left(\frac{bC_R}{K}\right)^2+\frac{\pi^2b^2}{6\omega^2}\right]C''+\ldots$$

$$+\frac{BKC'}{K^2+\omega^2C_R^2}(\omega C_R\cos\omega t-K\sin\omega t)+\ldots$$

while the cyclic (amplitude) measurement is

$$\tilde{C}=C\sqrt{}\Big\{1-\frac{2b\omega C_RK}{\omega(K^2+\omega^2C_R^2)}\frac{C'}{C}+\left(\frac{b}{\omega}\right)^2\frac{K^2}{K^2+\omega^2C_R^2}\left(\frac{C'}{C}\right)^2+\frac{2\pi^2}{3}\left(\frac{b}{\omega}\right)^2\frac{C''}{C}$$

$$+4\left(\frac{b}{\omega}\right)^2\frac{\omega C_RK}{K^2+\omega^2C_R^2}\frac{C''}{C}-\frac{4}{B}\left(\frac{b}{\omega}\right)^3\left(\cos\omega t+\frac{\omega C_R}{K}\sin\omega t\right)\frac{C''}{C} \tag{31}$$

$$-\frac{1}{2}\left(\frac{b}{\omega}\right)^2\frac{(K^2+\omega^2C_R^2)\cos 2\omega t+2\omega C_RK\sin 2\omega t}{K^2+\omega^2C_R^2}\frac{C''}{C}+\ldots\Big\}.$$

Due to the appearance of the linear term $\frac{2b\omega C_RKC'}{\omega(K^2+\omega^2C_R^2)C}$ in (31) the straightforward use of the cosine of the corrected phase angle does not help significantly in this case. (But note that errors in the cyclic measurement can be reduced by using a higher frequency.)

It can be observed that for the underlying measurement to be good the quantity C should change little over a temperature increase bC_R/K: $bC_R/K \ll C/C'$ or $K/bC_R \gg C'/C = \mathrm{d}\ \ln C/\mathrm{d}T$. For the cyclic measurement a high frequency guarantees a good estimate, even if the underlying (conventional) measurement is poor. For example, making $\omega/b \gg \mathrm{d}\ln C/\mathrm{d}T$ makes the third term inside the square root of (31) very small.

4. One-dimensional and three-dimensional calorimeters

Throughout this section the approach of §2.4 is adopted. This avoids having to obtain quite general solutions to coupled ordinary and partial differential equations.

To start with the interior of the calorimeter is thought of as a one-dimensional heat conducting medium, such as a metal bar, in which the heat equation holds. The two pans are represented by points on the bar which have positive heat capacity. The one-dimensional assumption means that explicit, albeit complicated, formulae can be obtained. In the last part of this section a more realistic three-dimensional configuration, for which explicit formulae are not general obtainable, is treated.

4.1 An inert sample on a uniform, three-section bar

To take a definite case the calorimeter is thought of as a bar of length $3l$ with ends $x=-l$ and $x=2l$. The end points take the block temperature T_F. The sample pan is located at $x=0$ and the reference is at $x=l$. This 1/3, 1/3, 1/3 division is only considered as one possible example. The analysis used here easily carries over to more general symmetric, and even asymmetric (and branched) cases, see §4.3 below.

At the pans there are no jumps in temperature

$$T=T_s \quad \text{at} \quad x=0 \quad \text{and} \quad T=T_R \quad \text{at} \quad x=l$$

and net heat flow gives the rate of change of temperature:

$$kS_b\left[\frac{\partial T}{\partial x}\right]_{0-}^{0+}=(C_R+C_s)\frac{\mathrm{d}T_s}{\mathrm{d}t}$$

and

$$kS_b\left[\frac{\partial T}{\partial x}\right]_{l-}^{l+}=C_R\frac{\mathrm{d}T_R}{\mathrm{d}t}.$$

Here k is the thermal conductivity and S_b the cross-sectional area of the bar. The sample temperature is programmed to be

$$T_s=T_o+bt+B\sin\omega t=T_o+bt+\mathrm{Im}\{Be^{i\omega t}\}$$

so it is possible to find T (and $T_R=T|_{x=l}$) in a similar form:

$$T = \overline{T}(x) + bt + \mathrm{Im}\{\widetilde{T}(x)\mathrm{e}^{\mathrm{i}\omega t}\}.$$

From the heat equation the somewhat simpler underlying part satisfies

$$\frac{\mathrm{d}^2\overline{T}}{\mathrm{d}x^2} = \frac{\rho cb}{k} \quad -l < x < 0,\ 0 < x < l,\ l < x < 2l,$$

where ρ=density and c=specific heat of the bar, and $\overline{T}$ has solutions

$$\overline{T} = \frac{\rho cb}{2k}x^2 + T_{\mathrm{o}j} - T_{1j}x$$

in the intervals

$$-l < x < 0\ (j = 1),\ \ 0 < x < l\ (j = 2)\ \text{ and }\ l < x < 2l\ (j = 3).$$

Looking at the requirements at x=0 gives

$$T_{\mathrm{o}1} = T_{\mathrm{o}2} = T_{\mathrm{o}} \ \text{ and } \ T_{12} - T_{11} = \frac{(C_{\mathrm{R}} + C_{\mathrm{s}})b}{kS_{\mathrm{b}}}.$$

The continuity of temperature and conservation of heat at x=l likewise yields

$$T_{\mathrm{o}3} + lT_{13} = T_{\mathrm{o}2} + lT_{12} \ \text{ and } \ T_{13} - T_{12} = \frac{C_{\mathrm{R}}b}{kS_{\mathrm{b}}}.$$

Finally, the fact that at both end points (x=$-l$ and x=$2l$) the temperature is the same (T_{F}) means that

$$T_{\mathrm{o}3} + 2lT_{13} - (T_{\mathrm{o}1} + lT_{11}) = -\frac{3\rho cbl^2}{k}.$$

There are now six equations for the six unknows $T_{\mathrm{o}j}$, T_{1j} and this linear system is easily solved. In particular it is found that

$$T_{12} = \frac{C_{\mathrm{s}}b}{3kS_{\mathrm{b}}} - \frac{\rho cbl}{2k}$$

and

$$\Delta\overline{T} = \overline{T}_{\mathrm{R}} - \overline{T}_{\mathrm{s}} = \left(\frac{\rho cb}{2k}l^2 + T_{\mathrm{o}2} + T_{12}l\right) - T_{\mathrm{o}2} = \frac{bl}{3kS_{\mathrm{b}}}.$$

The underlying measurement for heat capacity is then

$$\overline{C}_{\mathrm{s}} = \frac{3kS_{\mathrm{b}}}{bl}\overline{\Delta T}\,; \tag{32}$$

as with the ODE model the factor $3kS_b/bl$ can be found experimentally through calibration.

This prediction can be compared with that of the ODE model in Section 2. Taking this essentially steady situation (the rate of temperature rise and the temperature differences are constant for the underlying part), the effective heat-transfer coefficients between the two pans and each pan and the block (the closer end of the bar) can be seen to be $K_o=K_1=kS_b/l$ (using the notation of Section 2). (A temperature differential of θ over a section of bar length l results in a temperature gradient θ/l and consequent heat flow (θ/l) × cross-sectional area × thermal conductivity.) It follows that $K=K_o+2K_1=3kS/l$ and (32) is just (7).

Turning now to the cyclic part and again applying the heat equation, $\tilde{T}$ must satisfy

$$\frac{d^2\tilde{T}}{dx^2}=m^2\tilde{T} \text{ in each section } (j=1,2,3).$$

Here $m=(1+i)\beta$ with

$$\beta=\sqrt{\frac{\omega\rho c}{2k}}. \tag{33}$$

(This type of spatial variation was considered inside a "large" sample in [9].) The solutions are then

$$\tilde{T}=C_j e^{mx}+A_j e^{-mx} \quad j=1,2,3.$$

The six complex coefficients C_j and A_j are determined by using the conditions at the ends of the segments. Starting with $x=0$, the requirements that $T=T_s$,

$$\tilde{T}_s=\mathrm{Im}\{Be^{i\omega t}\}$$

and

$$\left[\frac{\partial T}{\partial x}\right]_{0-}^{0+}=\frac{(C_R+C_s)}{kS_b}\frac{dT_s}{dt}$$

give

$$C_1+A_1=C_2+A_2=B$$

and

$$(C_2-A_2)-(C_1-A_1)=\frac{i\omega(C_R+C_s)B}{mkS_b}.$$

The continuity of temperature and conservation of heat at $x=l$ yield

$$C_2e^{ml} + A_2e^{-ml} = C_3e^{ml} - A_3e^{-ml}$$

and

$$C_2e^{ml} - A_2e^{-ml} - C_3e^{ml} + A_3e^{-ml} = \frac{i\omega C_R(C_2e^{ml} + A_2e^{-ml})}{mkS_b}.$$

Finally, the fact that $\widetilde{T}(-l)=\widetilde{T}(2l)$ means that

$$C_1e^{ml} + A_1e^{-ml} = C_3e^{2ml} + A_3e^{-2ml}.$$

As with the underlying part it is now a matter at solving six linear equations for six unknowns; unfortunately the coefficients make the present system quite messy to solve on paper. Use of a computer algebra package (Maple) eventually results in

$$\widetilde{\Delta T} = \mathrm{Im}\left\{\left[(C_2e^{ml} + A_2e^{-ml}) - B\right]e^{i\omega t}\right\}$$

$$= \frac{C_sB\omega}{kS_b\beta}(q_c\cos\omega t + q_s\sin\omega t) = \frac{C_sB\omega}{kS_b\beta}\,\mathrm{Re}\left\{qe^{i\omega t}\right\} \tag{34}$$

where $q=q_c-iq_s$,

$$q_c = [(q_1 + q_2)q_3 + (q_2 - q_1)q_4]/q_D$$

$$q_s = \left[(q_1^2 + q_2^2)(C_R\omega/kS_b\beta) + (q_2 - q_1)q_3 - (q_1 + q_2)q_4\right]/q_D$$

$$q_D = [q_3 + (q_2 - q_1)(C_R\omega/kS_b\beta)]^2 + [q_4 - (q_1 + q_2)(C_R\omega/kS_b\beta)]^2 \tag{35}$$

$$q_1 = \cos 2l\beta\cosh 2l\beta - 1$$

$$q_2 = \sin 2l\beta\sinh 2l\beta$$

$$q_3 = 4(\cos l\beta\sinh l\beta + \cos 2l\beta\sinh 2l\beta)$$

and

$$q_4 = 4(\sin l\beta\cosh l\beta + \sin 2l\beta\cosh 2l\beta).$$

The amplitude of this cyclic part is

$$|\widetilde{\Delta T}| = \frac{C_sB\omega}{kS_b\beta}\,|q|$$

so the cyclic measurement is

$$\tilde{C}_s = \frac{kS_b\beta}{|q|}\frac{|\tilde{\Delta}T|}{\omega B} = \left(\frac{3kS_b}{l}\right)\left(\frac{\beta l}{3|q|}\right)\frac{|\tilde{\Delta}T|}{\omega B} = K\times\frac{\beta l}{3|q|}\times\frac{|\tilde{\Delta}T|}{\omega B}$$

with $K=3kS_b/l$.

Note that q is a function of βl and $C_R\omega/kS_b\beta=3/K\times C_R\omega/\beta l$, or equivalently, of βl and $C_R\omega/K$. Thus $\tilde{C}_s$ can be expressed as $(K|\tilde{\Delta}T|/\omega B)\times$ a calibration constant $(\beta l/3|q|)$ which depends upon $C_R\omega/K$ and βl.

The calibration constant differs from that for the simple ODE model of Section 2 in its complexity, and through its dependence upon $\beta l=\sqrt{\omega\rho c/2k}\,l$. For a fixed frequency ω it can be determined via calibration at that frequency. Since ω controls the calibration constant through βl and $C_R\omega/K$ two calibrating runs would be needed to fix this factor for all frequencies. It should be noted that this procedure relies on the precise form of q as given by (35). Other one-dimensional configurations (with different lengths, cross-section areas etc.) give rise to different functional forms. Given this uncertainly calibration should be done over a suitable range of frequencies and interpolation used as necessary.

The Eq. (34) for the cyclic part of the temperature can be alternatively written as

$$\tilde{\Delta}T = \frac{C_sB\omega}{K}\mathrm{Re}\left\{\frac{e^{i\omega t}}{P}\right\}$$

where $P=\beta l/3q$ takes the role of $1+i\omega C_R/K$ in the ODE model. The phase lag is now

$$\varphi = \varphi_b \equiv \tan^{-1}\frac{\mathrm{Im}\{P\}}{\mathrm{Re}\{P\}} = \tan^{-1}\frac{q_s}{q_c}.$$

4.2 A reacting sample on a uniform, three-section bar

Since the sample still has the set temperature $T_s=T_o+bt+\sin\omega t$ the concentration and the rate of absorption of heat by the reaction are as in Section 2 for the first-order reaction:

$$a \cong \tilde{a} \cong a_o\exp\left[\int_0^t g(T_o+bt)\mathrm{d}t\right]$$

and

$$f \cong r + Br'\sin\omega t$$

with $r=\bar{a}g(T_o+bt)$ and $r'=\bar{a}g'(T_o+bt)$.

Once again the complex heat capacity $C_s - ir'/\omega$ can be substituted for C_s to give, in place of (34),

$$\tilde{\Delta} T = \frac{B\omega}{kS_b\beta}\mathrm{Re}\left\{\left(C_s - \frac{ir'}{\omega}\right)q\mathrm{e}^{\mathrm{i}\omega t}\right\}$$

$$= \frac{B\omega}{K}\mathrm{Re}\left\{\frac{C_s - ir'/\omega}{P}\mathrm{e}^{\mathrm{i}\omega t}\right\}.$$

As before the cyclic measurement becomes

$$\tilde{C}_s = C_s\sqrt{1 + \left(\frac{r'}{\omega C_s}\right)^2}$$

which can be improved by multiplying by $\cos\varphi_c$, the corrected phase lag φ_c being given by

$$\varphi_c = \varphi - \varphi_b = \tan^{-1}\frac{r'}{\omega C_s}.$$

Thus the baseline subtraction method proposed by Reading [1] is also valid in this more sophisticated model.

4.3 One-dimensional generalizations

As mentioned above the same approach can be taken to find explicit formulae for the calibration factors (and phase lags) using other one-dimensional models for calorimeters. The complexity of the expressions increases with intricacy of the model but all typically involve trigonometric and hyperbolic functions of ratios of length scales (l) of components of the calorimeter to diffusion lengths ($\sqrt{k/\rho c\omega} = 1/2\beta$).

The simplest representation of all is to regard the two bars as being isolated from each other so that the calorimeter consists of two bars, each lying between $x=0$ and $x=l$, with the temperatures at $x=0$ both being T_F, one bar connected to the sample pan and having temperature T_s at $x=l$, and the other leading to the reference pan where the temperature is T_R [14].

The temperature in each pan satisfies the heat equation $\rho c\partial T/\partial t = k\partial^2 T/\partial x^2$. The configuration is sketched in Fig. 7.

Conservation of heat at the pans gives

$$kS\frac{\partial T}{\partial x}\bigg|_{x=l} + (C_R + C_s)\frac{\mathrm{d}T_s}{\mathrm{d}t} = 0$$

for the sample bar and

$$kS\frac{\partial T}{\partial x}\bigg|_{x=l} + C_R\frac{dT_R}{dt} = 0$$

for the reference bar.

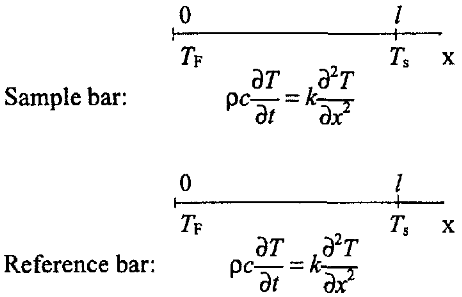

Fig. 7 Simple one-dimensional calorimeter: two bars leading from heat source at $x=0$ to the pans at $x=l$

For this system the problems for the temperatures in the pans can be considered in isolation, but using the fact that $T=T_F$ at $x=0$ for both.

Once again, on taking the usual T_s, the temperatures in the bars take the form

$$T = T_{0j} + T_{1j}x + \frac{\rho cbx^2}{2k} + \mathrm{Im}\{\tilde{T}_j(x)e^{i\omega t}\}$$

with

$$\tilde{T}_j = C_j e^{mx} + A_j e^{-mx};$$

where $j=1$ for the sample bar and 2 for the reference bar.

The constant T_{01}, T_{11}, C_1 and A_1 can be found using the two equations at $x=l$; they then fix T_F. Once T_F is known T_{02}, T_{12}, C_2, A_2 and T_R can be determined. The outcome is a version of (34) with a simpler version of (35).

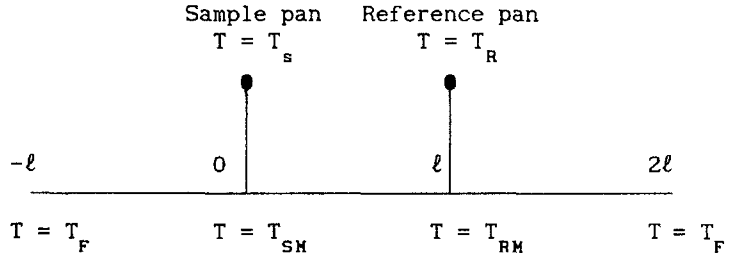

Fig. 8 One dimensional-calorimeter with thermal resistances

A more complicated model for the calorimeter regards it as a bar, as in §4.1 and §4.2, with the thermocouples 1/3 and 2/3 along, but with thermal resistances between those points and the pans (c.f. §2.5). The set-up is shown schematically in Fig. 8.

The differential equations are the same as in §4.1 but, even for an inert sample, the boundary conditions differ in that

$$\text{at} \quad x = 0 \qquad T = T_{\mathrm{SM}} = T_o + bt + B\sin\omega t$$

(measured and programmed temperature $\neq T_s$),

$$(C_{\mathrm{R}} + C_s)\frac{\mathrm{d}T_s}{\mathrm{d}t} = K_t(T_{\mathrm{SM}} - T_s) = kS_b\left[\frac{\partial T}{\partial x}\right]_{o-}^{o+}$$

(rate of increase of enthalpy of sample = rate of heat flow between $x=0$ and pan = heat transfer coefficient × temperature jump = jump in heat flow in bar);

$$\text{at} \quad x = l \qquad T = T_{\mathrm{RM}}, \qquad C_{\mathrm{R}}\frac{\mathrm{d}T_{\mathrm{R}}}{\mathrm{d}t} = K_t(T_{\mathrm{RM}} - T_{\mathrm{R}}) = kS_b\left[\frac{\partial T}{\partial x}\right]_{l-}^{l+}$$

Again putting $T=\bar{T}(x)+bt+\mathrm{Im}\{\tilde{T}(x)e^{i\omega t}\}$ and solving the resulting ordinary differential equations gives:

$$\text{for the underlying part, } \overline{\Delta T} = \text{constant} \times C_s;$$

$$\text{for the cyclic part, } \widetilde{\Delta T} = BC_s\mathrm{Re}\{\hat{T}e^{i\omega t}\},$$

where $\hat{T}$ involves trigonometric and hyperbolic functions (c.f. §4.1), but has in its numerator a factor $[1+i\omega(C_{\mathrm{R}}+C_s)/K_t]$ (c.f. (27)).

The same comment as in §2.5 applies: observations in real calorimeters give no indication of significant thermal resistance, $(C_{\mathrm{R}}+C_s)\omega/K_t$ is negligible, and the possibly troublesome factor reduces to a constant (e.g. 1).

Finally, in this subsection it is possible to look at biased devices. Asymmetry can result from the lengths, cross-sectional areas etc. of the two sections linking the pans to the block being different.

From all this variety of possibilities one specific case is considered here. This is like the simple two-bar representation at the start of this subsection, with identical cross-sections, densities, and thermal properties, but different lengths. The temperature difference $\Delta T=T_{\mathrm{R}}-T_s$ has an underlying part ΔT with similar properties to that for the biased ODE model (§2.5) and a cyclic part

$$\widetilde{\Delta T} = B\mathrm{Re}\{[C_s(M_1 + iM_2) + (M_3 + iM_4)]\}e^{i\omega t}.$$

The M's in this expression can be written in terms of trigonometric and hyperbolic functions with M_3 and M_4 vanishing when the bars have the same length. Now

$$|\tilde{\Delta T}| = B\sqrt{(M_1C_s + M_3)^2 + (M_2C_s + M_4)^2}$$

and the coefficients $(M_1^2+M_2^2)$, $2(M_1M_3+M_2M_4)$, $(M_3^2+M_4^2)$ can be fixed by carrying out three calibrations (over a suitable range at ω if necessary). The heat capacity for a subsequent sample can then be determined (on solving a quadratic equation).

4.4 Reduction to the ODE model

It was noted in §4.1 that the underlying measurement gave the same result as the discrete-mass model of Section 2. This can be thought of as resulting, at least in part, from the fact that the specific heat of the bar (representing the material of the actual calorimeter) plays only a minor role when the temperature is changing at a constant rate. The same is certainly not true for the cyclic part. The term ρc has a major effect on the heat equation for the oscillating temperature and hence on the q that appears in (34).

As the specific heat c decreases this term should get less important, the thermal mass of the calorimeter reduces in relation to those of the pans, and the model should become more like that of Section 2.

In fact it can be seen that the key parameter is βl (the ratio of the geometric and diffusion lengths). Taking $\beta l = l\sqrt{\omega\rho c/2k}$ tending to zero expression (35) for q reduces to

$$\frac{l\beta}{3}\times\frac{1}{1 + \mathrm{i}C_R\omega K}$$

with $K=3ks/l$. Then (34) is simply $\tilde{\Delta T} = B\omega C_s\mathrm{Re}\{\mathrm{e}^{\mathrm{i}\omega t}/(K+\mathrm{i}\omega C_R)\}$, that is (26) with no reaction.

Thinking of the bar as being made of Constantan, $\rho c \cong 4\cdot 10^6$ J K^{-1} m^{-3} and $k\cong 20$ W m^{-1} K^{-1}. Taking the period of modulation to be about 1 min, $\omega=2\pi/60 \cong 10^{-1}$ s^{-1}. The value of β is then approximately 100 m^{-1}. For a device with linear dimensions typically 1 cm, $l\beta$ is then close to 1.

If the calorimeter is significantly smaller, or the period longer, then $l\beta$ would be small.

(It should be noted that taking the cross-sectional area to be about 10^{-6} m^2, which is suggested by a thickness of 0.1 mm and, for a disc, a typical radius of 1 cm, K is of size 10^{-2} W K^{-1}. With a pan of heat capacity 10^{-2} J K^{-1} which is equivalent to 2.5 mg of a material with specific heat $4\cdot10^2$ J K^{-1} kg^{-1}, an angular frequency 10^{-1} s^{-1} makes $\omega C_R/K$ also about 1.)

4.5 A three-dimensional calorimeter

Quite general calorimeters (with two or three dimensions) can be examined in much the same way as the one-dimensional devices. The calorimeter may be thought of as a conducting medium surrounding the two pans which have surfaces S_s and S_R and temperatures T_s and T_R. The outer surface S_F of the calorimeter is, for the present, taken to have a uniform temperature

$$T_F = bt + \mathrm{Im}\{\hat{B}e^{i\omega t}\}.$$

The temperature in the enclosed region (but outside S_s and S_R) satisfies the heat equation

$$\rho c\frac{\partial T}{\partial t} = k\nabla^2 T.$$

The device is something like that indicated by Fig. 9.

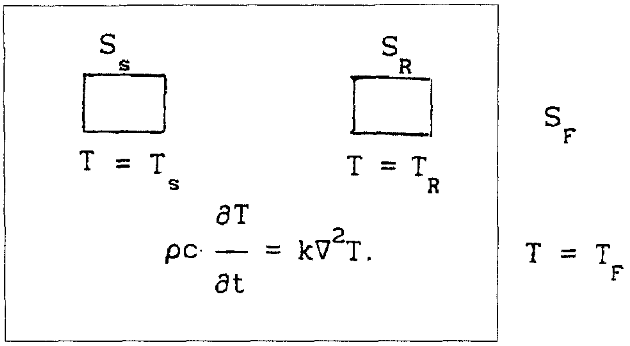

Fig. 9 Schematic diagram of a calorimeter

The usual procedure is followed and the temperature is written as

$$T = b\left(t + \frac{\rho c}{k}\bar{T}(x)\right) + \mathrm{Im}\{\hat{B}\hat{T}(x)e^{i\omega t}\},$$

in particular

$$T_j = b\left(t + \frac{\rho c}{k}\bar{T}_j\right) + \mathrm{Im}\{\hat{B}\hat{T}_j e^{i\omega t}\} \text{ for } j = R, S.$$

Balancing the rate of change of heat content of the pans with the heat flow in through their surfaces gives

$$C_R\frac{dT_R}{dt} = -k\int\limits_{S_R}\frac{\partial T}{\partial n}dS,$$

$$(C_R + C_s)\frac{dT_s}{dt} = -k\int\limits_{S_s}\frac{dT}{dn}dS.$$

Here $\partial/\partial n$ denotes the normal derivative out of the calorimeter (into the pans). Splitting into the underlying and cyclic parts gives

$$\frac{C_R}{\rho c} = -\int\limits_{S_R}\frac{\partial \overline{T}}{\partial n}dS, \quad \frac{C_R + C_s}{\rho c} = -\int\limits_{S_s}\frac{\partial \overline{T}}{\partial n}dS,$$

$$\frac{i\omega C_R\hat{T}_R}{k} = -\int\limits_{S_R}\frac{\partial \hat{T}}{\partial n}dS, \quad \frac{i\omega(C_R + C_s)}{k} = -\int\limits_{S_s}\frac{\partial \hat{T}}{\partial n}dS,$$

as well as having

$$\overline{T} = \overline{T}_R \text{ and } \hat{T} = \hat{T}_R \text{ on } S_R, \quad \overline{T} = \overline{T}_s \text{ and } \hat{T} = \hat{T}_s \text{ on } S_s,$$

$$\overline{T} = 0 \text{ and } \hat{T} = 1 \text{ on } S_F.$$

Additionally the differential equations

$$\nabla^2\overline{T} = 1 \text{ and } \nabla^2\hat{T} = i\Omega\hat{T} \text{ where } \Omega = \frac{\rho c\omega}{k},$$

must hold.

Both temperature variables can be written in three parts

$$\overline{T} = z_o + \overline{T}_R z_R + \overline{T}_s z_s \text{ where the } z\text{'s satisfy}$$

$$\nabla^2 z_o = 1 \text{ with } z_o = 0 \text{ on } S_F, S_R, S_s$$

$$\nabla^2 z_R = 0 \text{ with } z_R = 1 \text{ on } S_R \text{ but } z_R = 0 \text{ on } S_F, S_s$$

$$\nabla^2 z_s = 0 \text{ with } z_s = 1 \text{ on } S_s \text{ but } z_s = 0 \text{ on } S_F, S_R;$$

$$\hat{T} = w_F + \hat{T}_R w_R + \hat{T}_s w_s \text{ where the } w\text{'s satisfy}$$

$\nabla^2 w_j = i\Omega w_j$ with $w_j = 1$ on S_j and $w_j = 0$ on the other two parts of the boundary.

For a symmetric (unbiased) calorimeter:

$$-\int\limits_{S_R}\frac{\partial z_o}{\partial n}dS = -\int\limits_{S_s}\frac{\partial z_o}{\partial n}dS = \gamma_o > 0;$$

$$\int_{S_R}\frac{\partial z_R}{\partial n}\mathrm{d}S=\int_{S_s}\frac{\partial z_s}{\partial n}\mathrm{d}S\equiv\gamma_1>0;$$

$$-\int_{S_R}\frac{\partial z_s}{\partial n}\mathrm{d}S=-\int_{S_s}\frac{\partial z_R}{\partial n}\mathrm{d}S\equiv\gamma_2>0;$$

$$-\int_{S_R}\frac{\partial z_F}{\partial n}\mathrm{d}S=-\int_{S_s}\frac{\partial w_F}{\partial n}\mathrm{d}S\equiv\alpha_o;$$

$$\int_{S_R}\frac{\partial w_s}{\partial n}\mathrm{d}S=\int_{S_s}\frac{\partial w_R}{\partial n}\mathrm{d}S\equiv\alpha_1;$$

$$-\int_{S_R}\frac{\partial w_s}{\partial n}\mathrm{d}S=-\int_{S_s}\frac{\partial w_R}{\partial n}\mathrm{d}S\equiv\alpha_2. \tag{36}$$

The temperatures of the two pans can be found by solving the two pairs of linear equations

$$\frac{C_R}{\rho c}=\gamma_o-\gamma_1\bar{T}_R+\gamma_2\bar{T}_s$$

and

$$\frac{C_R+C_s}{\rho c}=\gamma_o+\gamma_2\bar{T}_R-\gamma_1\bar{T}_s\,;$$

$$\frac{\mathrm{i}\omega C_R\hat{T}_R}{k}=\alpha_o-\alpha_1\hat{T}_R+\alpha_2\hat{T}_s$$

and

$$\frac{\mathrm{i}\omega(C_R+C_s)}{k}=\alpha_o+\alpha_2\hat{T}_R+\alpha_1\hat{T}_s;$$

for $\bar{T}_R$, $\bar{T}_s$, $\hat{T}_s$ and $\hat{T}_s$.

The underlying part then satisfies

$$(\gamma_1+\gamma_2)(\bar{T}_R-\bar{T}_s)=\frac{C_s}{\rho c}$$

so the dimensional temperature difference is

$$\overline{\Delta T} = \frac{bC_s}{k(\gamma_1+\gamma_2)} = \frac{bC_s}{K}$$

for an effective heat-transfer coefficient $K=(\gamma_1+\gamma_2)k$.

The underlying measurement then takes the usual form

$$\overline{C_s} = \frac{K\overline{\Delta T}}{b}.$$

Turning to the cyclic part,

$$\frac{i\omega C_2\hat{T}_s}{k} = \left[(\alpha_1+\alpha_2)+\frac{i\omega C_R}{k}\right](\hat{T}_R-\hat{T}_s),$$

and the dimensional temperature difference satisfies

$$\widetilde{\Delta T} = \mathrm{Im}\{\hat{B}\Delta\hat{T}e^{i\omega t}\} = \mathrm{Im}\left\{\frac{Bi\omega C_s e^{i\omega t}}{(\alpha_1+\alpha_2)k+i\omega C_R}\right\},$$

taking the cyclic part of T_s to be $\tilde{T}_s=B\sin\omega t=\mathrm{Im}\{B\varepsilon^{i\omega t}\}$ as normal. Then

$$\widetilde{\Delta T} = B\omega C_s\mathrm{Re}\left\{\frac{e^{i\omega t}}{(\alpha_1+\alpha_2)k+i\omega C_R}\right\}. \tag{37}$$

This gives the standard results: the cyclic measurement of heat capacity is

$$\tilde{C}_s = \frac{|\widetilde{\Delta T}|}{B\omega}|(\alpha_1+\alpha_2)k+i\omega C_R|,$$

where $|\widetilde{\Delta T}|$ = amplitude of the temperature difference and $|(\alpha_1+\alpha_2)k+i\omega C_R|$ is a calibration factor, and there is a phase lag

$$\varphi = \varphi_b \equiv Arg\{(\alpha_1+\alpha_2)k+i\omega C_R\}$$

$$= \tan^{-1}\left[\frac{\omega C_R + k\mathrm{Im}\{\alpha_1+\alpha_2\}}{k\mathrm{Re}\{\alpha_1+\alpha_2\}}\right].$$

In principle the α's can be determined by numerically solving the boundary-value problem for w_R and evaluating (36) so the calibration factor and phase lag could be calculated for any given frequency ω. In practice it will be easier to find these two quantities from a calibrating run.

To calculate α_1 and α_2 it is necessary to find the complex scaled temperature $w=w_R$ which satisfies

$$\nabla^2 w = i\Omega w \ \left(\text{with } \Omega = \frac{\rho c\omega}{k}\right),\ w=1 \text{ on } S_R,\ w=0 \text{ on } S_F \text{ and } S_s.$$

The real and imaginary parts of $w=u+\mathrm{i}v$ can be determined from

$$\nabla^2 u + \Omega v = 0,\ \ \nabla^2 v = \Omega u,\ \ u = 1 \ \text{ and } \ v = 0 \text{ on } S_\mathrm{r},\ u = v = 0 \ \text{ on } S_\mathrm{F} \text{ and } S_\mathrm{s}.$$

Eliminating v gives

$$\nabla^4 u + \Omega^2 u = 0,\ \ u = 1 \ \text{ and } \ \nabla^2 u = 0 \ \text{ on } S_\mathrm{R},\ u = \nabla^2 u = 0 \ \text{ on } S_\mathrm{F} \text{ and } S_\mathrm{s}.$$

This model also reduces to the ODE case in certain circumstances. Taking Ωl^2 to be small, for l a typical distance in the calorimeter, w can be sought formally as

$$w = w_\mathrm{o} + \Omega \mathrm{i} w_1 + \Omega^2 w_2 + \dots .$$

If this power series is substituted into the differential equation and boundary conditions then:

$$\nabla^2 w_\mathrm{o}=0,\ \ w_\mathrm{o}=1 \text{ on } S_\mathrm{R},\ w_\mathrm{o}=0 \text{ on } S_\mathrm{F} \ \text{ and } \ S_\mathrm{s}, \text{ so } \ w_\mathrm{o} \text{ is precisely } z_\mathrm{R};$$

$$\nabla^2 w_1 = z_\mathrm{R} > 0 \ \text{ with } \ w_1=0 \text{ on } S_\mathrm{F},\, S_\mathrm{R} \ \text{ and } \ S_\mathrm{s} \text{ determines (in principle) } w_1$$

and makes it negative with $\partial w_1/\partial n \geq 0$ on all parts of the boundary. (The results about the signs of the w's come from the Maximum Principle for elliptic equations, see, for example [15].) Then

$$\alpha_1 = \int_{S_\mathrm{R}} \frac{\partial w}{\partial n} \mathrm{d}S \sim \int_{S_\mathrm{R}} \frac{\partial z_\mathrm{R}}{\partial n} \mathrm{d}S + \mathrm{i}\Omega \int_{S_\mathrm{R}} \frac{\partial w_1}{\partial n} \mathrm{d}S + \Omega^2 \int_{S_\mathrm{R}} \frac{\partial w_2}{\partial n} \mathrm{d}S + \dots$$

$$\sim \gamma_1 + \mathrm{i} m_1 \Omega + m_2 \Omega^2 + ,$$

with $m_\mathrm{j} = \int_{S_\mathrm{R}} \frac{\partial w_\mathrm{j}}{\partial n} \mathrm{d}S > 0$ for $j=1,2$. Likewise

$$\alpha_2 \sim \gamma_2 - i\Omega n_1 - \Omega^2 n_2$$

on writing $n_\mathrm{j} = \int_{S_\mathrm{R}} \frac{\partial w_\mathrm{j}}{\partial n} \mathrm{d}S > 0,\ j=1, 2.$

Then (37) becomes

$$\widetilde{\Delta T} = B\omega C_\mathrm{s} \mathrm{Re} \left\{ \frac{\mathrm{e}^{\mathrm{i}\omega t}}{(\gamma_1 + \gamma_2)k + \mathrm{i}\Omega(m_1 - n_1) + \Omega^2(m_2 - n_2) + \dots + \mathrm{i}\omega C_\mathrm{R}} \right\},$$

the cyclic measurement is

$$\widetilde{C}_\mathrm{s} = \frac{|\widetilde{\Delta T}|}{B\omega} \ \sqrt{\left[K + \Omega^2(m_2 - n_2)\right]^2 + [\omega C_\mathrm{R} + \Omega(m_1 - n_1)]^2}$$

$$=\frac{K|\widetilde{\Delta} T|}{B\omega}\sqrt{1+(\omega C_R/K)^2+2\Omega(m_1-n_1)\omega C_R/K....},$$

and the phase lag is

$$\varphi_b=\tan^{-1}\left[\frac{\omega C_R+\Omega(m_1-n_1)\ ...}{K\ ...}\right].$$

The results of Section 2 are recovered on taking $\Omega \to 0$.

Similar results are possible even taking the calorimeter to be inhomogeneous, so that $\rho(x)c(x)\partial T/\partial t=\nabla(k(x)\nabla T)$, the calorimeter to have convective as well as conductive heat transport, and it to have an outside boundary condition of the form $T=T_0(x)+tT_1(x)+\mathrm{Im}\{\hat{B}(x)e^{i\omega t}\}$ on S_F.

In Sections 2 to 4 the possible sources of error have been comprehensively reviewed. The general conclusions are that: the calibration method already described in the literature [3] should give reasonable results, provided there are many modulations over the course of a transition, i.e. the frequency is in some sense high; the deconvolution of the signals into reversing and nonreversing events should make sense; and the baseline subtraction procedure described above and in [1] will enable the in and out-of-phase components of the cyclic signal to be quantitatively calculated using the phase lag. Improving thermal conduction between the baseplate and the sample by use of helium as the purge gas will reduce errors especially as the modulation frequency is increased.

5. Phase transitions

In this last section some simple models for change of phase in the sample are considered in conjunction with the basic ODE representation of Section 2. The intention is to understand how latent heat (absorbed by the sample as it changes to its high temperature phase) affects both the underlying and cyclic measurements.

5.1 Polymer melting

A very simple model might be to regard the material as changing its specific heat (without any absorption of latent heat) over some temperature range, with the specific heat determined purely by the temperature. The outcome of an experiment is then as in Section 3 or, more simply, in §2.2 but evaluating C_s at $\bar{T}_s$: $C_s=C_s(T_0+bt)$.

A variation of this model to include the latent heat of fusion is possible. The sample might be thought of as mixture having a whole range of different molecular weights. There would then be some distribution describing the composition, for instance $Z(W)$=proportion, by mass, of the polymer with molecular weight $\leq W$. The polymer of molecular weight W is taken to have a melting point $T_c(W)$, with T_c in some bounded interval, say (T_1, T_2). Possible profiles of Z and T_c are sketched in Fig. 10.

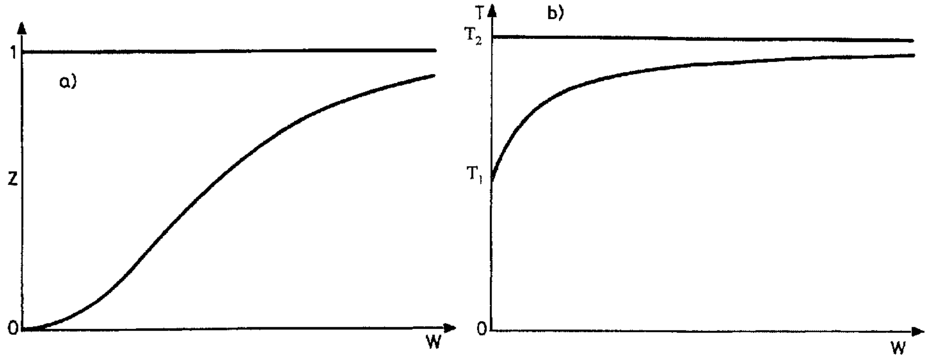

Fig. 10 Mass distribution (a) and melting point (b) against molecular weight

Supposing for simplicity that the specific heats of the crystalline material and melt are identical the amount of heat needed to increase the temperature of a sample of mass M from T to $T+\delta T$ is then $(c_s\delta T+L\ \delta Z)M$. The increment δZ might be taken to be given by $\delta Z = (\mathrm{d}Z/\mathrm{d}T)\ \delta T = h\delta T$, where h is the distribution function for the proportion of polymer with given melting point (Fig. 11).

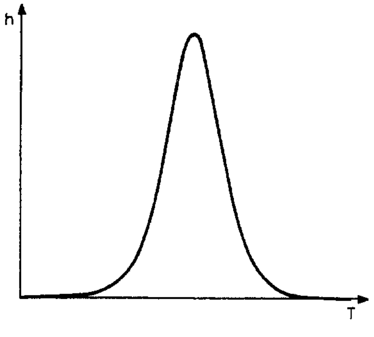

Fig. 11 Distribution of molecular weight with temperature

The heat input must then be $(c_s+Lh)M\delta T=C_s\delta T$, where $C_s(T)=(c_s+Lh)M$ is the effective heat capacity of the sample. In such a model the effect of the phase change is simply to increase the specific heat over the range of temperatures where the change occurs (Section 3).

The following models are more sophisticated and cannot be described by a temperature-dependent specific heat.

The case considered above was first articulated by Reading *et al.* [1] where it was observed that "If the crystallite melting temperatures have a distribution and they are able to melt rapidly without extensive superheating, something that would normally be true, then at least part of the MTDSC signal will be in phase with dT/dt as this determines the speed at which a fresh population of crystallites find themselves at their melting temperature." In this simple model, where no rearrangemetn occurs, all of the signal will be in phase with dT/dt and there will be no peak in the phase lag. There may be some polymers where this model holds because rearrangement is slow or non-existent. We will be considering the case where rearrangement occurs in a future publication.

5.2 Polymer crystallisation (the Avrami equation)

The Avrami equation is a model for crystallisation of a polymer and should ideally only be applied to cases of decreasing temperature, $b<0$.

The crystallinity of the sample (proportion of crystalline material), a, decreases with time and, using the form given in [16] and [17], is given by

$$a = 1 - \exp\left\{-\left[\int_{o}^{t} k_a(T_s)\mathrm{d}t\right]^{N}\right\}$$

where $k_a > 0$ is the crystallisation rate function or

$$a = 1 - \mathrm{e}^{-G_a^N}, \quad G_a^N = \int_{o}^{t} k_a(T_s)\mathrm{d}t.$$

The rate of heat release by the sample is

$$-f = LM\frac{\mathrm{d}a}{\mathrm{d}t} = NLMkG_a^{N-1}\mathrm{e}^{-G_a^N}.$$

The sample has, as usual, temperature $T_s = bt + B\sin\omega t$, and it is possible to proceed as in §2.3 and §2.4. The crystallisation rate function is linearized (separated into underlying and cyclic parts),

$$k_a = k_a(T_o + bt) + Bk'_a(T_o + bt)\sin\omega t + \ldots = \bar{k}_a + B\bar{k}'_a\sin\omega t + \ldots,$$

and the integral G_a is

$$G \cong \tilde{G}_a + B\tilde{G}_a$$

$$\text{with} \qquad \overline{G}_a = \int_{o}^{t} k_a(T_o + bt)\mathrm{d}t \text{ and}$$

$$\tilde{G}_a = \int_o^t k'_a(T_o + bt)\sin\omega t\,dt$$

$$\cong \frac{1}{\omega}(k'_a(T_o) - k'_a(T_o + bt)\cos\omega t) \text{ if } \omega \text{ is "large".}$$

Once again we are able to linearize quantities of interest through the supposition that B is sufficiently small. Splitting $-f$ into its underlying and cyclic parts gives

$$-f \cong NLMe^{-\overline{G}_a^N}\left\{\overline{k}_a\overline{G}_a^{N-1} + B\left[\overline{k}'_a\overline{G}_a^{N-1}\sin\omega t + \overline{k}_a((N-1)\overline{G}_a^{N-2} - N\overline{G}_a^{2(N-1)})\tilde{G}_a\right]\right\}$$

$$\cong NLM\overline{G}_a^{N-1}e^{-\overline{G}_a^N}(\overline{k}_a + B\overline{k}'_a\sin\omega t)$$

$$= r + Br'\sin\omega t$$

with $r = NLM\overline{k}_a\overline{G}_a^{N-1}e^{\overline{G}_a^N}$ and $r' = r\overline{k}'_a/\overline{k}_a$.. Here it has been assumed that ω is large enough for $\tilde{G}$ terms to be negligible.

It follows that

$$\overline{\Delta T} = \frac{1}{K}(bC_s - r) \quad \text{so} \quad \overline{C}_s = C_s - \frac{r}{N} \quad \text{(recall that } b < 0\text{)}$$

and

$$\tilde{\Delta T} = \omega B\mathrm{Re}\left\{\frac{C_s + ir'/\omega}{K + i\omega C_R}e^{i\omega t}\right\} \quad \text{so} \quad \tilde{C}_s = \sqrt{1 + (r'/\omega C_s)^2}.$$

The phase lag is

$$\varphi = \tan^{-1}\frac{\omega C_R}{K} - \tan^{-1}\frac{r'}{\omega C_s} = \varphi_b + \varphi_c$$

and can be used, as above, to give the improved estimate $\tilde{C}_s\cos\varphi_c$.

There is, therefore, a direct parallel between the kinetic process of a chemical reaction and the kinetic process of crystallisation [18]. Consequently the separation of the signal into reversing and nonreversing signals has the same meaning.

5.3 Melt of a pure material

The sample is taken to be a slab (a thin disc) so that it is essentially one-dimensional. It is taken to be symmetric which means that only one half need be considered. The surface of the material is $x=0$, and, for this preliminary work, is supposed to have the temperature T_s. The centre is $x=l_s$ (the width of the sample is $2l_s$) and, from the symmetry, the temperature gradient vanishes there: $\partial T/\partial x=0$ at $x=l_s$.

While the material is changing phase there is a free boundary, say $x=s_f(t)$, separating the crystalline material in $s_f<x<l$ from the melt in $0<x<s_f$, (Fig. 12).

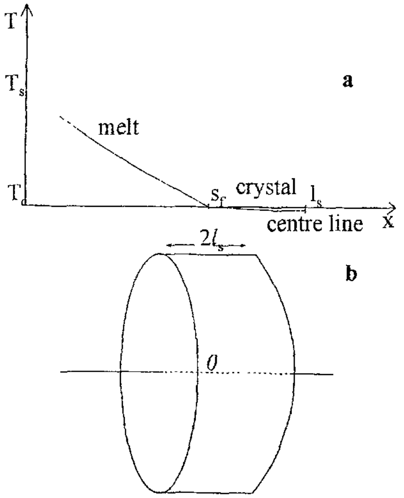

Fig. 12 Form the temperature profile across the sample during melting (a) and sample configuration (b)

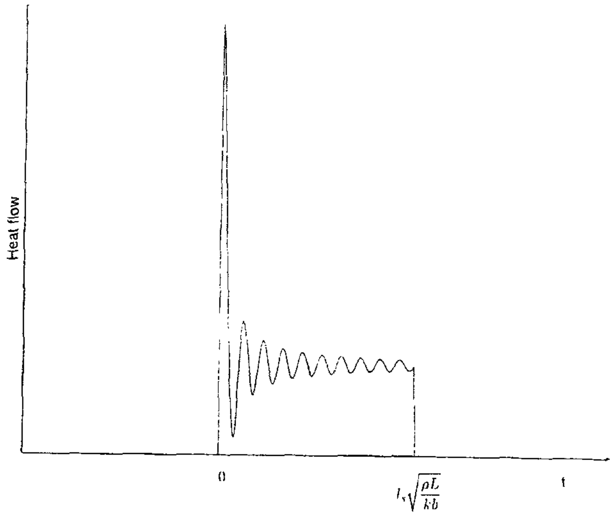

Fig. 13 Rate of heat flow into a melting sample for a simple one-dimensional Stefan model for the phase change

(As earlier, the actual scales change with the values of b, L etc. and are deliberately omitted from Figs 12 and 13; here we only indicate the qualitative behaviour.)

In the two parts the temperature satisfies the heat equation

$$\rho c\frac{\partial T}{\partial t}=k\frac{\partial^2 T}{\partial x^2}\quad 0<x<s_\mathrm{f}\quad\text{and}\quad s_\mathrm{f}<x<\mathrm{l}_\mathrm{s}.$$

For simplicity the density, specific heat, and thermal conductivity are all assumed to be constant but (given what will follow) it is quite easy to generalize this analysis to allow various properties to take different values in the two phases or even be more generally temperature dependent.

To simplify the notation the melting temperature of the sample is taken to be $T=T_\mathrm{c}$ and the time at which melting starts is $t=0$. The free boundary forms at $x=0$ when $t=0$ and moves towards l_s, reaching the centre when the phase change is complete. On $x=s_\mathrm{f}$ the temperature is meting, T_c, and the usual Stefan condition, accounting for the latent heat L, holds

$$k\left[\frac{\partial T}{\partial x}\right]_{s_\mathrm{f}-}^{s_\mathrm{f}+}=\rho L\frac{\mathrm{d}s_\mathrm{f}}{\mathrm{d}t}.\ \text{(The left hand side is } k\text{×jump in } \frac{\partial T}{\partial x} \text{ at } s_\mathrm{f}.\text{)}$$

To complete the specification of temperature an initial value (resulting from the run up to time zero) must be given and, for conventional DSC, the full Stefan problem for T is:

$$\rho c\frac{\partial T}{\partial t}=k\frac{\partial^2 T}{\partial x^2}\quad\text{in}\quad 0<x<s_\mathrm{f}\quad\text{and}\quad s_\mathrm{f}<x<l_\mathrm{s},$$

$$T=T_\mathrm{c}\quad\text{on}\quad x=s_\mathrm{f},\quad k\left[\frac{\partial T}{\partial x}\right]_{s_\mathrm{f}-}^{s_\mathrm{f}+}=\rho L\frac{\mathrm{s}_\mathrm{f}}{\mathrm{d}t},$$

$$T=T_\mathrm{s}=T_\mathrm{c}+bt\ \text{on}\ x=0,\quad \frac{\partial T}{\partial x}=0\quad\text{on}\quad x=l_\mathrm{s},\quad\text{and}$$

$$T=T_\mathrm{i}(x)\ \left(\equiv-\frac{\rho cb}{2k}\left[l_\mathrm{s}^2-(l_\mathrm{s}-x)^2\right]\le 0\right)\quad\text{at}\quad t=0.$$

(For a fuller treatment of Stefan problems see [19].)

To try to identify the important terms the problem is nondimensionalized. Distance is naturally scaled with the half-width l_s, $x=l_\mathrm{s}y$ and $s=l_\mathrm{s}s_\mathrm{d}$. Temperature and time should be scaled to get a balance in the controlling boundary condition at $x=0$ (this condition drives the temperature and melting) and, since the phase change is thought to be important, in the Stefan condition. Trying $T=T_\mathrm{c}+T_2\theta$ (T_2

is now the size of the change of temperature T_s during melting) and $t=t_2\tau$ (t_2=the time scale for this process), the two conditions become

$$T_2\theta = bt_2\tau \text{ on } y=0 \text{ and } \frac{kT_2}{l_s}\left[\frac{\partial\theta}{\partial y}\right]_{s_d-}^{s_d+} = \frac{\rho L l_s}{t_2}\frac{\mathrm{d}s_d}{\mathrm{d}\tau}.$$

All parameters can be eliminated from these two equations by choosing

$$t_2 = l_s\sqrt{\frac{\rho L}{kb}} \text{ and } T_2 = l_s\sqrt{\frac{\rho Lb}{k}}.$$

Using this scaling the nondimensional Stefan problem takes the form

$$\varepsilon_m\frac{\partial\theta}{\partial\tau} = \frac{\partial^2\theta}{\partial y^2} \text{ in } 0<y<s_d \text{ and } \text{in } s_d<y<1,$$

$$\theta = 0 \text{ on } y = S_d, \quad \left[\frac{\partial\theta}{\partial y}\right]_{s_d-}^{s_d+} = \frac{\mathrm{d}s_d}{\mathrm{d}\tau},$$

$$\theta = \tau \text{ on } y = 0, \frac{\partial\theta}{\partial y} = 0 \text{ on } y = 1, \text{ and}$$

$$\theta = \theta_i(y) = \frac{T_i}{T_2} \leq 0 \text{ at } \tau = 0.$$

Here $\varepsilon_m=\rho c l_s^2/t_2 k = c l_s\sqrt{\frac{\rho b}{kL}}$ is the Stefan number and, for sample sizes of interest, is generally very small (taking $c\cong 2\cdot 10^3$ J kg^{-1} K^{-1}, $l_s\cong 10^{-4}$ m, $\rho=10^3$ kg m^{-3}, $k\cong 0.2$ W m^{-1} K^{-1}, $L=6\cdot 10^4$ J kg^{-1}, $\varepsilon_m\cong 2\cdot 10^{-3}$): during the melting the specific heat is unimportant compared with the latent heat and the left-hand side of the heat equation can be neglected.

The reduced problem indicates that θ is linear for both $y<s_d$ and $y>s_d$. The latter in conjunction with $\theta=0$ on $y=s_d$ and $\partial\theta/\partial y = 0$ on $y=1$, means that $\theta=0$ for $s_d\leq y\leq 1$. (In particular $\theta=0$ at $\tau=0$; when only specific heat has to be accounted for the temperature variation within the sample is very small). Using the condition on $y=0$ gives $\theta = \tau(1-y/s_d)$ *for* $0\leq y\leq s_d$. Application of the Stefan condition yields a differential equation for s_d,

$$\frac{\mathrm{d}s_d}{\mathrm{d}\tau} = \frac{\tau}{s_d},$$

which integrates to give $s_d=\tau$ since $s_d=0$ at $\tau=0$. (Then $\theta = \tau - y$ for $0<y<s_d$.)

The solution is also, to leading order, the leading approximation to the underlying part of the solution for MTDSC. Returning to dimensional variables the temperature is $T=T_c$ for $s_f \le x \le l_s$ and

$$T = T_c + bt + B\sin\omega t - \frac{x}{s_f}(bt + B\sin\omega t) \text{ for } 0 \le x \le s_f.$$

The free boundary is controlled by

$$\frac{ds_f}{dt} = \left(\frac{k}{\rho L}\right) \times \frac{bt + B\sin\omega t}{s_f}$$

which means that

$$s_f^2 = \frac{k}{\rho L}\left[bt^2 + \frac{2B}{\omega}(1 - \cos\omega t)\right]$$
$$\text{or } s_f \cong \sqrt{\frac{kb}{\rho L}}\left[t + \frac{B}{\omega bt}(1 - \cos\omega t)\right] \tag{38}$$

if B is sufficiently small for us to be able to linearize. (For the time derivative of the temperature still to be negligible $\varepsilon_m \times$ dimensionless frequency must be small: $\omega c\rho l_s^2/k=10^{-2} \ll 1$ taking $\omega=0.1\ s^{-1}$ and the earlier values for c, ρ, l_s, and k. It can be noted that there is a singularity at $t=0$ in (38). This results from B/ω not being small compared with bt^2 at the start of melting.)

Taking the cross-sectional area of the sample to be S_c its mass is $2\rho S_c l_c$. For $t<0$ it is inert, $C_s=2\rho S_c l_s c$, and likewise for $t>t_2=l_s\sqrt{\rho L/kb}$. In these two periods, before and after melting, the underlying and cyclic measurements (according to Section 2, (7) and (8)) give $\overline{C_s}=\tilde{C}_s=C_s$.

During the melting period the rate of intake of heat is approximately

$$2\rho S_c \frac{ds_f}{dt} L \cong 2S_c\sqrt{kb\rho L}\left[1 + \frac{B}{bt}\left(\sin\omega t - \frac{1}{\omega t}(1 - \cos\omega t)\right)\right].$$

(Terms of size ε_m and contributions from specific heat are still regarded as being unimportant). Melting takes time t_2 so ωt has a typical size $\omega t_2=l_s\omega\sqrt{\rho L/kb}$. If the frequency is still assumed to be high, in the sense that many cycles occur over the melting interval, $\omega t_2 \gg 1$ and the term $(1-\cos\omega t)/\omega t$ can be neglected. Then the rate of heat flow into the sample is

$$\frac{dQ_s}{dt} \cong 2S_c\sqrt{kb\rho L}\left(1 + \frac{B\sin\omega t}{bt}\right).$$

The basic ODE model is approximately

$$C_R \frac{d\Delta T}{dt} + K\Delta T = 2S_c\sqrt{kb\rho L}\left(1 + \frac{B\sin\omega t}{bt}\right).$$

The usual procedure results in the temperature difference

$$\Delta T = \overline{\Delta T} + \widetilde{\Delta T} = \frac{2S_c\sqrt{kb\rho l}}{K} + \frac{2BS_c}{t}\sqrt{\frac{k\rho L}{b}}\frac{(K\sin\omega t - \omega C_R\cos\omega t)}{K^2 + \omega^2 C_R^2}$$

and heat-capacity values

$$\bar{C}_s = 2S_c\sqrt{\frac{k\rho L}{b}},\quad \tilde{C}_s = \frac{2S_c}{\omega t}\sqrt{\frac{k\rho L}{b}};$$

for $0 < t < t_2$ (Fig. 14).

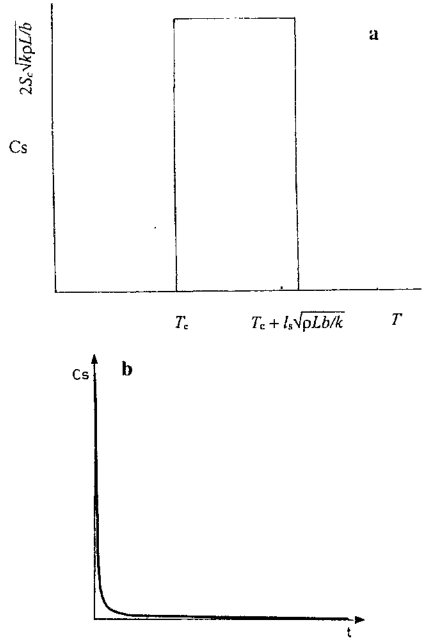

Fig. 14 Plots of underlying (a) and cyclic (b) measurements of heat capacity against temperature T_s

From the assumption of "high frequency", $\omega t \gg 1$ for the bulk of the duration of the change of phase so $\tilde{C}_s \ll \bar{C}_s$. Of course the area of the rectangular hump in the $\bar{C}_s - T$ plot is $\bar{C}_s T_2 = 2l_s S_c \rho L =$ mass of sample × latent heat. Better estimates of $\bar{C}_s$ and $\tilde{C}_s$, including the effect of specific heat, will be found by getting a more accurate solution for T in the sample as an asymptotic series in powers of the Stefan number, ε_m.

The above model assumes that the base of the sample can be forced to follow the imposed temperature programme. (The same assumption is made in all of the analysis presented here.) In practice, for pure materials such as indium, the sample cannot follow the programme, thus the above analysis does not apply. We shall be considering this in a future article.

6. Summary

Our analysis of a heat flux DSC cell under modulated-temperature conditions reveals that quantitative data on heat capacities can be obtained using the simple calibration methods that have already been described, [3]. It also demonstrates that the method of correcting for instrumental factors when exploiting the phase lag to divide the cyclic signal into in and out of phase components proposed in [1] is well founded and this conclusion is supported by experimental evidence. Our analysis describes how, when an irreversible chemical reaction or crystallisation occurs, it is possible to separate out the contributions made to the total heat flow by the heat capacity the (reversing contribution) and the enthalpy of the reaction or crystallisation (the non-reversing contribution). We have presented the first steps toward a more general analysis of phase transitions and will be presenting a further analysis of the glass transitions and real polymer melting behaviour in the near future.

Notation

a	(remaining) mass fraction of reactant or crystalline material
a_0	initial mass fraction
b	temperature ramp
c	specific heat capacity
f	rate of heat intake by a kinetic process within the sample
g	temperature-dependence function of a reaction rate
h	distribution function for molecular weights
k	thermal conductivity
k_a	function appearing in the Avrami equation
l	length scale of a (one-dimensional) calorimeter
l_s	half-width of a sample
m	complex spatial-decay rate of modulated temperature
m_j	coefficients in a power series for α_1 (j=1,2,...)
n	outward normal
n_j	coefficients in a power series for α_2 (j=1, 2,...)
p	order of a reaction
q, q_j	coefficients appearing in expressions for $\widetilde{\Delta T}$ (j= C, S, D, 1, 2, 3, 4)

r	reaction rate
r'	temperature derivative of reaction rate
s	time used in integrations
s_d	dimensionless position of a free boundary
s_f	position of a free boundary
t	time
t_2	time scale of melting
u	real part of w
v	imaginary part of w
$w=w_R$, w_s, w_F	functions of position determining $\hat{T}$
w_j	coefficients in power series w (j=0, 1, 2...)
x	position within calorimeter or sample
y	dimensionless position
z_o, z_R, z_s	functions of position determining $\bar{T}$
A	pre-exponentional rate constant
A^*	adjusted pre-exponential rate constant
A^+	scaled pre-exponential rate constant
A_j	coefficients appearing in expressions of cyclic temperature in region j (j=1, 2, 3)
B	amplitude of modulation of temperature
$\hat{B}$	complex amplitude of temperature (a complex multiple of B)
B_j	complex amplitude of T_j (j=F, R, S, RM or SM)
$C(T)$	heat capacity of the sample when it depends up on temperature
C_R, C_s	heat capacities of pan and sample
C_j	coefficients appearing in expressions of cyclic temperature in region j (j=1, 2, 3)
$\bar{C}_s$	value of sample's heat capacity given by underlying "measurement"
$\tilde{C}_s$	value of sample's heat capacity given by cyclic "measurement"
D	heat capacity of sample regarding it as a function of σ
E	activation energy
F, G	functions of time appearing in a nearly periodic signal
F_M, $\bar{G}_M$, $\tilde{G}_M$,	"measured" versions of F, G
G_a	function appearing in the Avrami equation
H	heat of reaction
I	function of time appearing in a nearly periodic signal
$\bar{I}_M$, $\tilde{I}_M$	"measured" versions of I
K	effective heat-transfer coefficients
K_t, K_o, K_1, K_2	internal heat-transfer coefficients
L	latent heat
M	mass of sample
M_j	coefficients in expressions for $\widetilde{\Delta T}$ (j=1, 2, 3, 4)
N	exponent appearing in the Avrami equation

P	coefficient appearing an $\tilde{\Delta}T$
Q_R, Q_s	heat contents of reference pan, sample pan plus sample
R	gas constant
S	a surface
S_b	cross-sectional area of a bar
S_c	cross-sectional area of a sample
S_F	external surfaces of calorimeter
S_R, S_s	surfaces of reference and sample pans
$\underset{\sim}{T}$	temperature
T	scaled complex amplitude of modulated temperature
$T_i(x)$	temperature on initiation of melting
T_c	melting temperature
T_e	external temperature
T_F, T_R, T_s	temperatures of furnace, reference, sample
T_{RM}, T_{SM}	temperatures measured for reference and sample
T_o	initial temperature
T_a, T_1, T_2	typical temperatures
T_{oj}	initial values of T_j(j=F, R, S, RM, SM)
T_{oj}, T_{1j}	coefficients appearing in expressions for underlying temperature in region j of a one-dimensional calorimeter (j = 1,2,3)
ΔT	temperature difference, $T_R - T_s$
ΔT_j	coefficients in a power series of ΔT(j = 0,1,2,...)
U	dimensionless temperature based on reaction rate
W	molecular weight
$Z(W)$	mass fraction with molecular weight $\leq W$
α	scaled amount of reactant
α_j	surface integrals of normal derivatives of w's (j = 1,2,3)
β	spatial decay rate of modulated temperature
γ_j	surface integrals of normal derivatives of z's (j = 1,2,3)
δ	dimensionless temperature over which $C(T)$ varies
ε	1/ dimensionless activation energy
ε_m	Stefan number
η	error in measurement of temperatures due to location of thermo-couples
λ	degree of bias
ρ	density
σ	rescaled dimensionless temperature
τ	dimensionless time
φ	phase lag
φ_b, φ_c	baseline and corrected phase lags
φ_s	phase of alternative "reference" signal, e.g. furnace modulation

ψ	ratio indicating importance of ωC_R compared with K ("departure from perfection")
θ	dimensionless temperature
θ_i	dimensionless temperature on initiation of melting
ω	angular frequency of modulation of temperature
Ω	rescaled angular frequency
$\bar{\ }$	underlying part (not C's, F's, G's, I's)
$\tilde{\ }$	cyclic part (not C's, F's, G's, I's)
$'$	derivative with respect to argument (not r)

References

1 M. Reading, D. Elliot, and V. L. Hill, "Some aspects of the theory and practice of modulated differential scanning calorimetry", Proc. 21st North American Thermal Analysis Society Conference, 1992, p. 145-150.
2 M. Reading, Trends Polymer Sci., 1 (1993) 248.
3 M. Reading, A. Luget, and R. Wilson, Thermochim. Acta, 238 (1994).
4 M. Reading, R. Wilson and H. M. Pollock, in Proceedings of the 23rd North American Thermal Analysis Society Conference, 1994, p. 2–10.
5 B. Wunderlich, Y. Jin and A. Boller, Thermochim. Acta, 238 (1994) 277.
6 J. Hatta, Jpn. J. Appl. Phys., 33 (1994) 686.
7 B. Wunderlich and A. Boller, Abstract, 24th NATAS Conference, 1995.
8 J. E. K. Schawe, Thermochim. Acta, 261 (1995) 183.
9 S. M. Marcus and M. Reading, "Method and apparatus for thermal conductivity measurements", U.S. Patent 5335993, 1994.
10 J. D. Murray, Asymptotic Analysis, Oxford University Press, 1973.
11 E. J. Hinch, Perturbation Methods, Cambridge University Press, 1991.
12 B. Wunderlich, A. Boller, I. Okazaki and S. Kreitmeier, Thermochim. Acta, 283 (1996) 143.
13 K. J. Jones, I. Kinshott, M. Reading, A. A. Lacey, C. Nikolopoulos and H. M. Pollock, "The origin and interpretation of the signals of MTDSC", preprint.
14 S. Marcus, Private communication
15 M. H. Protter and H. F. Weinberger, Maximum principles in differential equations, Prentice-Hall, Englewood Cliff, N. J., 1967.
16 K. Nakamura, T. Watanebe, K. Katayama and T. Amano, J. Appl. Polym. Sci., 16 (1972) 1077.
17 K. Nakamura, K. Katayama and T. Amano, J. Appl. Polym. Sci., 17 (1973) 1031.
18 K. A. Q. O'Reilly and B. Cantor, Proc. Roy. Soc. Lon. A, 452 (1996) 2141.
19 J. Crank, Free and moving boundary problems, Oxford University Press, 1984.